Technological improvements in energetic efficiency and sustainability in existing combined-cycle gas turbine (CCGT) power plants

Antonio Colmenar-Santos*[a], David Gómez-Camazón[a], Enrique Rosales-Asensio[b], Jorge-Juan Blanes-Peiró[c]

[a]*Department of Electric, Electronic, Control, Telematic and Chemical Applied to Engineering, Technical School of Industrial Engineering UNED Juan del Rosal, 12 Ciudad Universitaria, 28040, Madrid, Spain*
[b]*Departamento de Física. Universidad de La Laguna. Avenida Astrofísico Francisco Sánchez S/N 38206, S/C de Tenerife. Spain*
[c] *Departamento de Ingeniería Eléctrica y de Sistemas y Automática, Escuela Técnica Superior de Ingenieros de Minas de LEÓN, Spain*

Abstract

Data from an existing combined-cycle gas turbine (CCGT) power plant are used to create a computer simulation to allow efficiency and emission calculations, simulation and assessing improvements that apply partial regeneration with solar hybridization. The proposed amendments to this triple-pressure steam-reheat combined cycle (CCC_{3PR}) with 400 MW of net power incorporates a regenerator and thermal energy, from a source of renewable solar energy up to 50 MW, in order to reduce the energy loss in the gas turbine. The calculation and simulation models were created using Visual Basic code. Regeneration and solar hybridization were found to contribute to increasing efficiencies of around 2.25% to 3.29% depending on the loading point. The reduction of gas consumption was between 6.25% and 9.45% and the overall cycle efficiency loss is minimal due to hybridization. There was a loss of the net power of the new cycle but it is considerably lower if than heat from a renewable source is supplied to the cycle. This net power loss has an average value of 7.5% with regeneration only and of 1% with regeneration and hybridization. The reduction of fuel consumption is significant which could result in saving approximately 4 million €/year. Partial regeneration in the gas turbine and solar thermal power in the existing CCGTs provide an interesting possibility for reducing emissions (by 26,167 t/year). In conclusion, partial regeneration with solar hybridization provides an interesting and proven possibility to increase performance and efficiency whilst reducing emissions from the existing CCC_{3PR}.

Keywords: Combined cycle, Gas Turbine, Regenerator, Efficiency analisys, Solar hybridization.

* Corresponding author. Tel.: +34 913 987 788; fax: +34 913 986 028.
E-mail addresses: acolmenar@ieec.uned.es (A. Colmenar-Santos),

Nomenclature

Symbols

APP	approach point,[-]
BP	low pressure,[-]
c_p	sprecific heat, kJ/(kg·K)
c	Cost, €
dT	temperature difference, K
e	Exergy, kJ/kg
h	entalpy, kJ/kg
HP	high pressure,[-]
I_e	irreversibility, W
LEC	levelized cost, €
$\dot{m}$	mass flow, kg/s
$\dot{m}_a$	mass flow rair, kg/s
$\dot{m}_G$	mass flow exhaust gases, kg/s
$\dot{m}_{v,IP}$	mass flow steam IP, kg/s
$\dot{m}_{v,AP}$	mass flow steam AP, kg/s
$\dot{m}_{v,BP}$	mass flow steam BP, kg/s
$\dot{m}_r$	mass flow reheater steam, kg/s
$\dot{m}_{extrac.}$	mass flow extraction steam, kg/s
p	pressure, bar
LHV	lower heating value, kJ/kg
PP	Pinch point, K
$\dot{Q}_{gases}$	mass flow exhaust gases, kg/s
r_c	compression ratio, [-]
s	Entropy, kJ/(kg·K)
T	Temperature, K
$TAT_{HP,BP}$	after turbine temperature, K
$TIT_{HP,BP}$	inlet turbine temperature, k
$T_{sal,\ BP,IP,AP}$	steam turbine temperature BP,IP,AP, K
ΔT	terminal difference temperatures, K
u	internal energy, kJ/kg
U	heat-transfer coefficient, ($W\cdot K^{-1}\cdot m^{-2}$)
UA	UA factor, ($W\cdot K^{-1}$)
$\dot{W}$	power,W

Greek Letters

α	recuperative mass fraction, [-]
ε	effectiveness of the regenerator, [-]

Subscripts and Acronyms

a	air
amb	ambient conditions
AP	high pressure level
atm	atmospheric pressure
BP	low pressure level
CCC	Combined cycle power plant
CCC_{3PR}	triple pressure HRSG with reheating
$CCC_{3PR,\ reg}$	CCC_{3PR} with regenerator
$CCC_{3PR,\ reg\&HS}$	$CCC_{3PR,\ reg}$ with solar hibridization
CCP	Parabolic cylindrical collector
CComb	combustion chamber
Comp	compressor
Cond.	condensator
CN	carnot factor
DSG	direct steam generation
in	inlet
ext	extraction steam turbine
exh	exhaust gases
ECO	economizer
EV	1ª combustor chamber GT
EVA	evaporator
f	fuel
F	Dosing
FW	feedwater
gen	generator
G	gas
GT	gas Turbine
GT26	gas turbine Alstom GT26
HTF	heat transfer fluid
HRSG	heat recovery steam generator
IP	intermediate pressure level
ISCC	integrated solar combined cycle
LFR	linear fresnel reflectors
out	out
P	pump
Rh	reheater

Υ	specific heat relation, [-]	Ref	reference
η	efficiency, %	reg	regenerator
$\eta_{is,C}$	isentropic efficiency compressor, %	sat	saturation
$\eta_{m,C}$	mechanic efficiency compressor, %	SC	steam cycle
$\eta_{m,T}$	mechanic efficiency turbine, %	SEV	2ª combustor chamber GT
$\eta_{m,bombas}$	mechanic efficiency pumps, %	SH	superheater
$\eta_{is,GT}$	isentropic efficiency compressor, %	ST	steam turbine
$\eta_{m,GT}$	mechanic efficiency gas turbine, %	TQ	tank
$\eta_{is,TV}$	isentropic efficiency steam turbine, %	Turb	turbine
$\eta_{m,TV}$	mechanic efficiency steam turbine, %	V	steam
η_{cc}	efficiency combined cycle, %	VGV	variable geometry blades
		0	reference conditions

1. Introduction

In the search of an efficient, economical and environmentally friendly energy, there is a clear shift towards renewable energy sources and decreasing emissions. This is an on-going process and the final solution has clearly not yet been reached [1][2].

Present day operating conditions of Combined-Cycle Gas Turbine (CCGT) power plants differ from the base load design conditions (approximately 400 MW), and therefore require performance studies and technological improvements at loading points others than the base load. This research considers practical improvements that can be made inside the existing CCGT plants operating in Spain and how these improvements can be implemented on the system operation conditions achieving emissions and fuel consumptions reductions and improving the system global efficiency. These changes will be in-line with Horizon 2020 directive [1][2][3]. It is necessary to include novelty improvements to give a response to these clean energy needs inside the existing CCGTs. In this aspect, the improvement of partial regeneration in gas turbine is possible. It is vital to advance research and development projects that deal with the emerging technologies that are needed to achieve these goals. Solar energy is another alternative, because it presents a great number of advanced technological options, such as the solar thermal power of concentration and its hybridization with conventional CCGTs. This is why the idea is to study the partial regeneration without or with the environmental benefits of solar energy inside the existing conventional combined cycle plant with steam turbine and gas turbine. This paper presents a computer-based model that compares the performance of three configurations of a CCGT: i) baseline, ii) CCGT + regenerator -to improve the gas-turbine efficiency-, and iii) CCGT + regenerator + heat from a solar thermal plant to increase the efficiency of the steam turbine. Comparisons are performed for different loading points to reflect the operating conditions of these plants as load-following resources. Firstly, the model CCGT was obtained. Then simulation results are compared with actual process data. The validation of the new models, with only partial regeneration and with regeneration and solar hybridization, was developed based on a design dataset of the existing CCGT in the four loading points once validated the CCGT model with the real one. In this way, the dataset, which comprises measurements of thermodynamic properties such as mass flows, temperatures, and pressures at key points in the system, can be validated under equal conditions. The thermal power introduced in the steam cycle, up to 50 MW, should be a power easily assumable by the existing cycle without the need to change equipment. The incognita in the new configuration will be to know how much is the maximum that can be absorbed and the best place.

Our goals are to demonstrate that this technical solution is feasible and to quantify the possible advantages. More specifically, we intend (i) to establish the limits within the regenerator and hybridization could work; (ii) to study the irreversibility that both improvements introduce, and finally, (iii) to assess the new sustainability in emissions and the performance improvements that would be obtained. All this is proposed maintaining the conventional layout of the plant and the same operation values in each of the studied loading points inside de existing CCGT.

In the first section, we offer an overview of the existing problem in current combined cycles. Section 2 presents the theoretical background on which the research was based, while in section 3 the materials and adopted methods are described. In chapter 4, the results of the techno-economic study and environmental impacts of the improvements are showed and discussed, and finally, conclusions are listed.

2. Theoretical Background

The modern CCC_{3PR} type combined-cycle power plants can easily reach efficiencies above 55%. ABB-Alstom claims an efficiency of 58.5% for a combined-cycle plant built around their GT24/26 reheat gas turbines [3][4]. In the technical literature, increased thermal efficiency of theoretical combined cycles is widely discussed [5][6][7][8][9][10][11], demonstrating the need of using regeneration and post-combustion in gas turbines. Another way proposed by Carcasci et

al. [12] was to study gas turbine technologies of high pressure ratio and of sequential combustion with a steam of cooling recovered in the heat recovery steam generator (HRSG). The comparison revealed that the gas turbine GT26, also studied in this work, uses consolidated technology with lower investment expenditure and that it is impossible to reach efficiencies higher than 60% in CCGT.

According to Bassily [13][14][15], sequential combustion with recuperator was introduced into a $CCC_{3PR,\ reg}$ varying the temperature inside the gas turbine (TIT). The results indicate that this cycle is 3.3 to 3.in% higher in efficiency than CCC_{3PR} at the same value of TIT. Air/steam blade cooling in the gas turbine increases TIT over 1500 ºC and the efficiency can be 0.64 to 1.19 percentage point higher.

In Sanjay Mohopatra [16], the impact of two different methods of inlet air cooling was compared in a combined cycle with cooled gas turbine (vapor compression versus vapor absorption cooling). They observed that vapor compression cooling improves the efficiency of gas turbine cycle by 4.88%, whereas in the case of vapor absorption cooling the efficiency improvement was 9.47%. For combined cycle configuration, however, vapor compression cooling should be preferred over absorption cooling due to higher plant performance. Other works and advances in this sense are [17][18].

The utilization of heat from the turbine cooling was studied in Kotowicz et al. [19]. The results indicated that by introducing the additional steam cycle, an efficiency growth of 2 to 3 % is gained, although this results in a corresponding increase in the compression ratio.

In Polyzakis et al. [20], four different gas turbine cycles (simple cycle, intercooled cycle, reheated cycle and intercooled and reheated cycle) were described and compared for the optimization of a combined-cycle power plant. The results showed that the reheated gas or sequential combustion gas turbine is the most desirable overall, mainly because of its high turbine exhaust gas temperature and resulting high thermal efficiency of the bottom steam cycle.

Similarly, in Rovira et al. [21], authors proved the convenience of using recuperative gas turbines for the dual pressure configurations and, especially, partial recuperation for both dual and triple pressure configurations. In almost all cases the optimal recuperative mass fraction was located at roughly 90%. In triple pressure level configurations, as in our case, fully-recuperative gas turbines are not advisable but the performance and cost may be improved if the gas turbine is partially recuperative.

Finally, in Gogoy et al. [22][23] the performance of a recuperated CCGT with fuel and air recuperator is compared to a non-recuperated CCGT and a CCGT with only air recuperator. Results reveal that heat recuperation from the exhaust gases is a suitable method to heat the air at the compressor and also the fuel entering into the combustion chamber. In Cao et al. [24] the differences between a CCGT and an Organic Rankine Cycle with an optimum design are discussed together with thermodynamic analysis of the gas turbine.

In a scenario of continuous and necessary rise of renewable energy use, cutting edge research must provide the know-how to integrate renewable energy sources into national electric generation plans and within the existing infrastructure network. Colmenar-Santos et al. [25]. This study considers the introduction of solar power, of 50 MW, provided by any of the technologies that currently exist in the market (such as parabolic cylindrical collectors/parabolic through collector (CCP/PTC), linear Fresnel reflectors (LFR) or solar tower (ST)) to be introduced into thermal systems for electricity production by heat transfer fluids (HTF). In this technology, solar collectors are cooled by an intermediate heat transfer fluid inside the troughs or steam can be produced directly within the troughs, (Direct Steam Generator, DSG).

The heat contributed by solar technologies can be integrated into an electricity production system by means of the so-called combined cycle. The combined cycle uses two turbines, one of steam in the Rankine cycle and another one of gas in the Brayton cycle. This residual heat produced in the gas turbine, at temperatures in the order of 550 °C, plus the heat supplied by the solar field, are used to power the steam turbine. This technology is known as ISCC (Integrated Solar Combined Cycle) [26][27][28][29][30][31][32][33][34].

A thorough technical literature review demonstrated that the ISCC technology is completely admissible today and there is a general agreement regarding the advantages of the integration of combined cycles and concentrating solar power. ISCC power plants have been widely studied as an alternative to the conventional arrangement of CCGT in localized places with high solar irradiation during all year. The contribution of solar thermal power to improve the performance of CCGTs is analyzed in our study, in order to assess the potential of this technique and know the maximum amount of thermal power, also the place of the Rankine cycle where must be introduced, that could be absorbed by the existing [35].

This configuration allows lower fossil fuel consumption and lower CO_2 emissions than conventional combined cycles, as well as a reduction in use of local and renewable resources [26][35][36]. Moreover, ISCCs reach higher solar thermal efficiency conversion than conventional solar thermal power plants. The reasons behind this are discussed in detail in [37][38][39][40] through case studies of plants with different technologies in different places, all of these with high solar irradiation . .

The thermal power is introduced in an existing CCGT, HTF or DSG by adding the steam in parallel with the steam produced in the HRSG. In the steam cycle, the solar heat is used to preheat or evaporate water of the high pressure level (as in our case) or of the intermediate level [40][41][42][43][44][45]. Additionally, the solar energy could be used to superheat steam with solar thermal oil and combustion gases, in a dual pressure steam generator [46]. Results showed that although Levelized Electricity Costs (LEC) were high in the year 2000 and depended considerably on the size of

the solar field, hybrid solar thermal power plants (ISCCS) may be competitive against conventional fuel fired power plants and CC.

The use of LFR could be possible for the low pressure level of the boiler [47]. An increase in power generation capacity of about 10% was observed by using solar thermal energy for feedwater heating and low pressure steam generation (LFR solar plant would replace one of the two HRSG).

Comparing HTF and DSG technologies, all results agree that DSG is the best evaporative option since it benefits both from low irreversibility at the heat recovery steam generator and high thermal efficiency in the solar field.

In relation to the comparison of the different technologies proposed in this present work, studies of Popov et al., Rovira et al. and Spelling et al.[48][49][50] are referenced, where LFR, ST and CCP are respectively described. Results show that the thermal contribution is higher with CCP than with LFR and it may improve the economic feasibility of the plant.

Therefore, ISCCs or the modified CCGT may be optimal choices since integrated designs may lead to a very efficient use of the solar and fossil resources [51]. Other studies related to the above comparing different configurations and types of plants are the studies of [52][53][54].

In spite of all that has already been discovered in the subject of efficiency improvements within the Rankine-Brayton cycle and of the recommended use of a regenerator coupled to the gas turbines, this solution has not yet been commercially considered in any operative CCC_{3PR} plants because of the normal operation in this type of power plants, until 2010, it was always in the upper loading limit point (400 MW). For this, it is necessary to have the maximum temperature at the inlet of the boiler and therefore contradictory and not necessary to make a by-pass of the exhaust gases of the gas turbine.

In addition, most of the improvements up to date have been obtained for low compression ratios and TIT values that are much higher than the working values of the current CCGTs.

The improvements of flexibility in the CCC_{3PR}, have also resulted in a loss of performance and efficiency, which increases as we move away from the design point (full load 400MW).

There are several setbacks that have impeded the integration of the described improvement in the CCC_{3PR}. The exhaust gas stream temperature decrease at the regenerator outlet would reduce the performance of the steam cycle and consequently that of the overall combined cycle. The regenerator would introduce more irreversibility and complexity to the gas turbine, due to having an exchanger with two currents with different heat capacities. Finally, the CCC_{3PR} was designed to operate on full load, which is very far from the current work conditions between loading limits 170 MW to 401 MW. This negatively affects the performance and the emissions.

In order to analyze and compare the conventional configuration to improved alternatives, multiparametric thermodynamic optimization was carried out in others studies maximizing the thermal efficiency [55][56][57].

The effect of the regeneration was predicted including an estimation of the new equipment and the exergetic losses that are introduced by the regenerator and the current of steam coming from the theoretical heat solar steam generator [58][59][60].

An exergy thermodynamic analysis of the new combined cycle (ISCC) reveals that the largest exergy losses occur in the combustor and the regenerator introduces more exergy losses in the gas and steam cycles [61][62]. This is the reason why the gas turbine should be carefully optimized, particularly by introducing measures to reduce the fuel consumption and emissions. Using this approach, the recuperation is advisable.

The currently operational combined cycle plants considered in this study are composed of a sequential combustion gas turbine, variable geometry in the high temperature cycle and a HRSG with reheating in the low temperature cycle. The union of both cycles allows a high global efficiency with high compression ratios (r_c) [3][4].

The efficiency of the gas turbine can be expressed as a function of the difference of work, between the gas turbine and the steam turbine, taking into account the supplied thermal power, (see equation (1)).

The efficiency of the whole CCC_{3PR} plant can be expressed as a function of the power of the gas turbine and the steam turbine and of the supplied thermal power taking into account the thermal heat provided by solar hybridization, $\dot{Q}_{solar}$, (see equation (2)). If the heat supplied is null would mean that there is regeneration in the gas turbine.

The first stage of the proposed configuration is a partial regeneration within the gas turbine. It consists of the thermal recuperation of a small portion of the total exhaust gas mass flow. This preheats the air exiting from the compressor. The exhaust gas mass that is not directed to the recuperator goes to the high temperature heat exchangers (superheaters and reheaters).

It is well known that the recuperative gas turbines include an additional heat exchanger (recuperator) that preheats the air coming from the compressor, using the exhaust gas coming from the turbine, which thereby allows some fuel saving and improves the performance and efficiency of the gas turbine. In this way, the amount of fuel in the EV chamber is reduced and the gas turbine efficiency increases.

As explained above, the reason why this improvement has not been yet considered is that the turbine exhaust temperature decreases during the recuperation process, which leads to an exergy decrease of the hot stream directed to the HRSG. Therefore, the quality of the produced steam decreases and, consequently, the efficiency of the steam cycle and ultimately that of the combined cycle is negatively affected.

A second technological improvement could be the introduction of thermal heat from a source of solar energy either by DSG or HTF technologies. The feasibility of this improvement is studied at each of the loading points. The aim of this modification is to compensate the described power loss induced by the regenerator of the gas turbine.

$$\eta_{GT} = \frac{\dot{W}_{turbine,GT} - \dot{W}_{compressor,GT}}{(\dot{m}_{EV} + \dot{m}_{SEV}) \cdot LHV} \quad (1)$$

As previously mentioned, the cycles currently in operation in the field are far from under full load working conditions. They operate at intermediate loading points above a minimum value set by the gas turbine manufacturer at around 170 MW. Under part load conditions, partially regenerative gas turbine technology could be an interesting solution in the combined cycle.

$$\eta_{CCC3PR} = \frac{\dot{W}_{GT} + \dot{W}_{ST}}{(\dot{m}_{EV} + \dot{m}_{SEV}) \cdot LHV + \dot{Q}_{solar}} \quad (2)$$

It must be mentioned that the operation of the modelled cycle, with and without regenerator, was compared at different loading points. For the study of this regenerator it was necessary to establish an exhaust gas stream, α, and the rest of the gas stream, 1-α, that goes directly to the HRSG.

Fig. 1 shows the layout of the configuration. As observed, the gas flow at the outlet of the turbine is divided into two streams. A fraction of the gas goes to the recuperator, whilst the remainder is directed to the HRSG. The stream circulating through the recuperator pre-heats the air coming from the compressor before it is introduced into the first combustion chamber. The other part of the exhaust gas goes to the HRSG, which has a non-conventional layout, particularly in the high-pressure part. Here, the vapor produced in the solar field and the steam produced in the HRSG are united. Also, the 1- α current joins the α current coming from the regenerator, once it has performed the heat exchange with the air stream at the outlet of the gas turbine compressor, prior to the EV stage.

The introduction of the regenerator and the fraction of exhaust gases, α, will make the efficiency of the gas turbine and the cycle vary for each of the considered points of charge (mass flow EV decrease). At this point it will be interesting to see the effect of the effectiveness of the regenerator, ε, which value is usually around 0.5% to 0.95% (an intermediate value of 0.7 has been used for calculations as a representative value in the parametric study). Thus, we can move from a conventional combined cycle (α = 0), to a fully recuperative gas turbine within the combined cycle (α = 1). Hence the proposed configuration is a combined cycle with partially recuperative gas turbine (0 < α < 1).

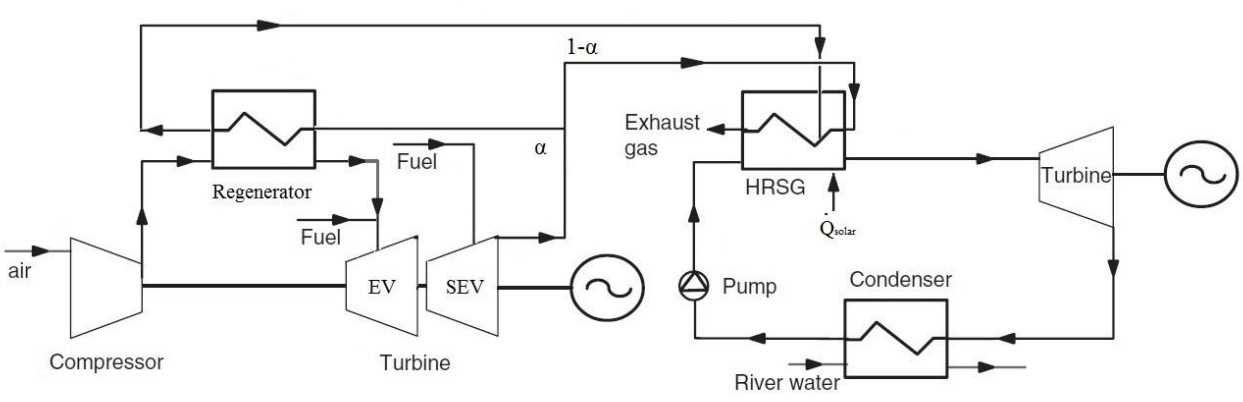

Fig. 1. Layout of the $CCC_{3PR\&HS}$ with partially regenerative regenerator and solar hybridization in HRSG by own elaboration.

On the other hand, due to the integration of the regenerator, the HRSG is divided into two zones: one of high temperature with the current 1-α, including only superheaters (SB) of high pressure (AP) and the reheater (RH); and the other one of low temperature composed of the economizers, evaporators and superheaters of the intermediate and low pressure levels. At the inlet of this zone, streams α and 1- α are mixed. This is the reason why the new mixing zone will have a point of exergetic loss where the alpha variation parameter must be applied. The same thing happens where the vapor, produced by the solar field, is mixed with the flow of steam generated in the high-pressure evaporator.

Configurations with triple pressure level and reheat (3PR), as is our case, are usually installed at high power charges

(approximately 400 MW net load on generator terminals). Fig. 2 shows the layout of the HRSG. It is important to evaluate how the regeneration affects the steam cycle due to the temperature decrease of the exhaust gases in fraction α.

The previous analysis has clearly proved that the key element to obtain an efficiency increase within the combined plant, is to increase the efficiency of the gas turbine. In most gas turbines, used for combined-cycle plants, the temperature of the turbine exhaust gas is higher (for GT26, it is 920 K) than required for the optimization. Therefore, the coupling of a HRSG and a regenerator can be a convenient strategy to increase the efficiency of the gas turbine when a sufficiently high temperature is available (higher than 823 K [7]).

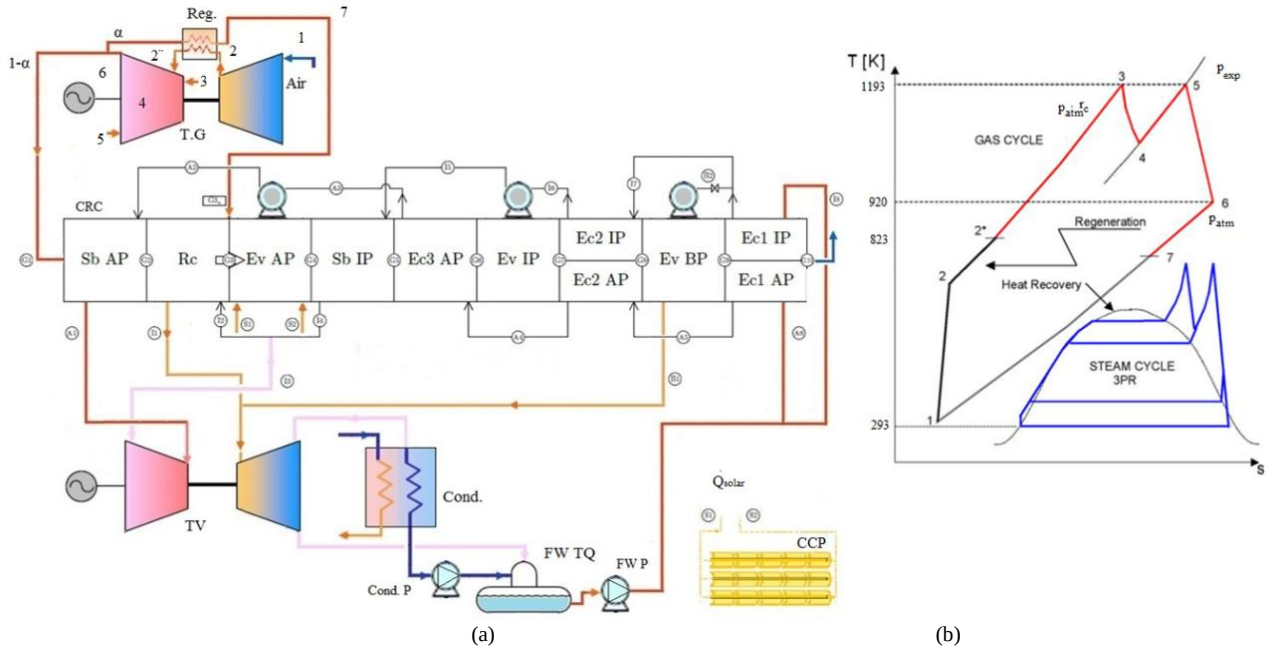

Fig. 2: (a) Detailed layout of the HRSG in the CCC_{3PR} with partially regenerative regenerator and solar hybridization in AP; (b) T-s diagram of the Brayton gas turbine and the Rankine steam cycle in 3PR configuration. (Own elaboration).

In this study, partial regeneration in the GT26 gas turbine and possible solar hybridization are proposed in the CCC_{3PR} at different loading points. Our goals are to demonstrate and quantify, inside the study of the three different configurations, the possible advantages. More specifically: (i) to establish the limits within which the regenerator and hybridization could work; (ii) to study the irreversibility that both introduce, and finally, (iii) to assess the performance improvements that would be obtained in the new regenerative combined cycle, with the possibility of absorbing a solar thermal power, up to 50 thermal MW. All this is proposed whilst maintaining the conventional layout of the plant and keeping the same operation values in each of the studied loading points.

A mathematical formulation code of each component of the real and the proposed cycles has been created in Visual Basic to assess the global performance of the new cycle. These include efficiency, exergy losses, fuel depletion ratio, irreversibility ratio, heat ratio, incremental solar efficiency, thermal efficiency and improvement potential. The component modeling is based on mass and energy balance, whereas thermal and thermodynamic proprieties are estimated using dll libraries of the program (pointGas pointWater).

An exergy thermodynamic analysis was also carried out comparing the existing CCC_{3PR} and the new models.

3. Materials and Methods

This paper presents a computer-based model that compares the performance of three configurations of a CCGT: i) baseline (existing CCGT), ii) CCGT + regenerator -to improve the gas-turbine efficiency-, and iii) CCGT + regenerator + heat from a solar thermal plant to increase the efficiency of the steam turbine. Comparisons are performed for different loading points to reflect the operating conditions of these plants as load-following resources.

Based on the fundamentals of thermodynamics and relations, the following comparative studies have been completed: (i) comparison of gas turbine cycle and steam cycle; (ii) comparison of a partially regenerative combined cycle with solar contribution, ($CCC_{3PR,reg\&HS}$) and a non-recuperated CCC_{3PR}; and (iii) comparison of exergetic losses.

Thermodynamic optimization was applied to the multiparametric analyses and to the comparative study maximizing the thermal efficiency of the new combined cycle.

The configuration of the two designs are shown in detail, where the most reliable model, verified by the conventional CCC_{3PR}, actually in operation, was used as a reference. The new improvements were incorporated into the reference

model and, after verification, its evolution was studied at four specific loadings points. This was by means of a parameterization study in order to increase the efficiency and global performance of the new combined cycle.

A computer simulation was developed using Visual Basic Code in order to allow simulation of the existing CCP_{3PR} cycle with real data and to then compare it with the improved $CCC_{3PR,reg\&HS}$ model. The theory was to obtain computer models in different parts of the cycles and the way to resolve the material and energy balances by iteration is shown in Appendix A.

The parameters of the gas turbine and the main design parameters of the HRSG and of the steam cycle of the conventional CCC_{3PR}, at each of the four loadings points, are shown in Table 1.

For these points, with the main base parameters of the HRSG and main data of gas turbine GT26, the possible variations during the analysis (range and limits) of the alpha parameter, α, and the amount of power mass heat inside the HRSG, Q, were assessed. The main data and values at each of the loading points were not modified during the analyses and further optimizations, in order to minimize degrees of freedom during the study.

To achieve the most reliable model of the current CCC_{3PR}, at each of the four loading points, it was necessary to introduce losses (i.e. performance, efficiency and pressure drops), in each component of the combined cycle.

The software calculated by iterations and loops, taking into account losses, pressure drops, etc.., the fuel consumption in each of the SEV and EV chambers. The charge regulation was carried out keeping the exhaust temperature constant. The obtained values were compared to the real ones in order to assess the reliability and fit of the model.

The PointWater and PointGas objects of the Visual Basic dll library (Dynamic-Link Library) were used for the object oriented programming of the model. The program provides properties of air, gas type and generated exhaust gases that could be easily adapted to the data obtained in the existing CCC_{3PR}, for given working conditions (loading points).

The objects created from the PointGas class were used to define the working points of the gas cycle, both for air and gas. These objects contain the necessary information to calculate the required air or gas properties and transformations.

For the resolution of the models, material and energy balances were applied for each of the cycles (i.e. gas turbine and steam cycle with solar thermal power), in order to obtain a correct coupling. As mentioned, real data of the cycle were used as design values in the models, in order to obtain the most realistic solutions possible. Due to difficulties presented by the large number of design parameters (see Table 1 and Table 2) and the complexity of the software that simulates the different configurations, four points have been chosen within the regulation limits in which the combined cycles currently work. Only four charging points were chosen, among the infinities that are within the limits of regulation, because they are enough to see the trends in addition to not complicate too much the parametric study. The multiparametric analyses and comparative study of the models consisted of varying the α fraction in the regenerator so that the software solved the material and energy balance of the cycle. It then compared the efficiencies and the rest of parameters, between the two models, maintaining the verified working values constant at each loading point.

It was also necessary to propose material balances in different parts of the cycle for each of the loading points (see Fig. 2 and data bases in Table 1 and Table 2) in order to establish mutual relations for the resolution of the models , one with regeneration and another with regeneration and solar hibridization, in the computer program by iteration (the mass flows of steam in each one of the three pressure levels).

The differences between the baseline and improved configurations can be found for different values of α mass fraction, in the first configuration improved, and α mass fraction and Q power mass heat for the second one, by the resolution of the model using the material and energy balances in each of the sections (see system equations 13).

Table 1: Parameters defining CCC_{3PR}, at each of the four loading points (minimum load 170 MW to full load 400 MW), by own elaboration with combined cycle data base from energy company EDP.

Input parameters at loading point 173 MW		**Input parameters at loading point 284 MW**	
Ambient temperature ($T_{amb\ ºC}$)	0.1	Ambient temperature ($T_{amb\ ºC}$)	5.1
Compressor ratio (r_c)	18.8	Compressor ratio (r_c)	23
Atmospheric pressure ($P_{atm\ mbar}$)	989	Atmospheric pressure ($P_{atm\ mbar}$)	993
Isoentropic efficiency compressor ($\Pi_{i,c}$) GT26	0.655	Isoentropic efficiency compressor ($\Pi_{i,c}$) GT26	0.725
Isoentropic efficiency turbine ($\Pi_{i,t}$) stage EV and SEV	0.95/0.965	Isoentropic efficiency turbine ($\Pi_{i,t}$) stage EV and SEV	0.93/0.935
Effectiveness of regenerator GT26 ($\varepsilon_{reg\ \%}$)	0.7	Effectiveness of regenerator GT26 ($\varepsilon_{reg\ \%}$)	0.7
Inlet compressor temperature ($T_{IN,\ Comp\ ºC}$)	473	Inlet compressor temperature ($T_{IN,\ Comp\ ºC}$)	499
Inlet gas turbine temperature EV($T_{IN,\ EV\ ºC}$)	1138	Inlet gas turbine temperature EV($T_{IN,\ EV\ ºC}$)	1123
Out gas turbine temperature EV ($T_{out,\ EV\ ºC}$)	950	Out gas turbine temperature EV ($T_{out,\ EV\ ºC}$)	947
Inlet gas turbine temperature SEV($T_{IN,\ SEV\ ºC}$)	1103	Inlet gas turbine temperature SEV($T_{IN,\ SEV\ ºC}$)	1234
Out gas turbine temperature SEV ($T_{out,\ SEV\ ºC}$)	591	Out gas turbine temperature SEV ($T_{out,\ SEV\ ºC}$)	640
Mechanic efficiency compressor ($\Pi_{i,c}$) TG	0.87	Mechanic efficiency compressor ($\Pi_{i,c}$) TG	0.95
Mechanic efficiency gas turbine ($\Pi_{i,t}$) TG	0.97	Mechanic efficiency gas turbine ($\Pi_{i,t}$) TG	0.96
VGV´s (º)	-41.4	VGV´s (º)	-28.2
Mass air rate ($m_{a\ kg/s}$)	361	Mass air rate ($m_{a\ kg/s}$)	457
LHV (kJ/kg)	48000	LHV (kJ/kg)	48000
Terminal difference temperature GAS-SH MP (K)	5	Terminal difference temperature GAS-SH MP (K)	5
Pressure level AP (bar)	67	Pressure level AP (bar)	93
Pressure level MP (bar)	14.7	Pressure level MP (bar)	20.2
Pressure level BP (bar)	3.2	Pressure level BP (bar)	3,2
Input parameters at loading point 348 MW		**Input parameters at loading point 401 MW**	
Ambient temperature ($T_{amb\ ºC}$)	3.8	Ambient temperature ($T_{amb\ ºC}$)	5.8
Compressor ratio (r_c)	26.5	Compressor ratio (r_c)	30
Atmospheric pressure ($P_{atm\ mbar}$)	989	Atmospheric pressure ($P_{atm\ mbar}$)	989
Isoentropic efficiency compressor ($\Pi_{i,c}$) GT26	0.765	Isoentropic efficiency compressor ($\Pi_{i,c}$) GT26	0.795
Isoentropic efficiency turbine ($\Pi_{i,t}$) stage EV and SEV	0.93/0.94	Isoentropic efficiency turbine ($\Pi_{i,t}$) stage EV and SEV	0.89/0.92
Effectiveness of regenerator GT26 ($\varepsilon_{reg\ \%}$)	0.7	Effectiveness of regenerator GT26 ($\varepsilon_{reg\ \%}$)	0.7
Inlet compressor temperature ($T_{IN,\ Comp\ ºC}$)	511	Inlet compressor temperature ($T_{IN,\ Comp\ ºC}$)	528
Inlet gas turbine temperature EV($T_{IN,\ EV\ ºC}$)	1117	Inlet gas turbine temperature EV($T_{IN,\ EV\ ºC}$)	1110
Out gas turbine temperature EV ($T_{out,\ EV\ ºC}$)	945	Out gas turbine temperature EV ($T_{out,\ EV\ ºC}$)	941
Inlet gas turbine temperature SEV($T_{IN,\ SEV\ ºC}$)	1270	Inlet gas turbine temperature SEV($T_{IN,\ SEV\ ºC}$)	1280
Out gas turbine temperature SEV ($T_{out,\ SEV\ ºC}$)	637	Out gas turbine temperature SEV ($T_{out,\ SEV\ ºC}$)	619
Mechanic efficiency compressor ($\Pi_{i,c}$) TG	0.94	Mechanic efficiency compressor ($\Pi_{i,c}$) TG	0.97
Mechanic efficiency gas turbine ($\Pi_{i,t}$) TG	0.96	Mechanic efficiency gas turbine ($\Pi_{i,t}$) TG	0.98
VGV´s (º)	-16.6	VGV´s (º)	2
Mass air rate ($m_{a\ kg/s}$)	518	Mass air rate ($m_{a\ kg/s}$)	591
LHV (kJ/kg)	48000	LHV (kJ/kg)	48000
Terminal difference temperature GAS-SH MP (K)	5	Terminal difference temperature GAS-SH MP (K)	5
Pressure level AP (bar)	104	Pressure level AP (bar)	116
Pressure level MP (bar)	23,2	Pressure level MP (bar)	26.5
Pressure level BP (bar)	3,4	Pressure level BP (bar)	4.1

Table 2: Additional HRSG 3PR (a) and gas turbine (b) parameters used in the models by own elaboration with combined cycle data base from energy company EDP.

Input parameters HRSG	
High pressure pinch point (PP_{AP})	7 K
High pressure approach point (APP_{AP})	4 K
High pressure AP temperature steam (T_{AP})	838 K
Medium pressure IP pinch point (PP_{MP})	5 K
Medium pressure IP approach point (AP_{MP})	6 K
Terminal temperature difference GAS-SH MP (K) ($\Delta T_{SB,MP}$)	5 K
Terminal temperature difference GAS-RH MP (K) ($\Delta T_{RC,MP}$)	5 K
Low pressure BP pinch point (PP_{BP})	5 K
Low pressure BP approach point (AP_{BP})	6 K
Pressure condensation (P_{cond})	50 mbar
Pressure extraction (P_{ext})	1.2 bar
Pressure desgasificator (P_{desg})	200 mbar
Isoentropic efficiency steam turbines AP/IP/BP ($\eta_{is,TV}$)	0.85
Mechanic efficiency pumps (ηis,pump)	0.75

(a)

Input parameters TG GT26	
Efficiency combustor chamber gas EV/SEv turbine (η_{ccomb})	98%
Pressure drop compresion (ΔP_{comp})	11%
Pressure drop exhaust (ΔP_{exh})	2%
Pressure drop regenerator air side (ΔP_{reg})	5%
Expansión relation ($P_{SEV/EV}$)	0.54

(b)

4. Results and Discussion

Next in this section, each of the proposed configurations will be analyzed and discussed in order to see the possible improvements that would be introduced in the existing cycle and under equal conditions. Three configurations in the existing CCGT are discussed: i) baseline (existing CCGT), ii) CCGT + regenerator -to improve the gas-turbine efficiency-, and iii) CCGT + regenerator + heat from a solar thermal plant to increase the efficiency of the steam turbine.

4.1. Thermodynamic analysis performance with only regeneration in the gas turbine

A mathematical model with the highest possible accuracy was developed to represent both the original CCC_{3PR} and the improved configurations. The performance improvements were studied and compared by means of parameter variation analysis.

The results of the multiparametric analysis reveal the comparison of efficiency of the two cycles under the same conditions at four loading points. These four loading points represent the usual working range of the current combined cycles with a regulation limits between a technical minimum, 170 MW, and full load, approximately 400 MW. Our goal was to find the most optimal loading point for the partial regeneration and to establish the maximum amount of thermal power (last configuration) that the new CCGT could absorb in order to obtain the maximum thermal efficiency in the global cycle. In this section the results of the different studies are showed.

Thermodynamic analysis of performance with regeneration only in the gas turbine shows the design parameters, limits and the main results of the parametric study. The study was carried out for zero recuperative mass fraction in the real cycle, between the upper and lower limits, and with partial recuperation, where the computer simulation program resolves correctly the material and energy balance. The limits, for which the regenerator can be introduced in GT26, are very extreme and are a direct function of the effectiveness (ε). For this case an ε value of 0.7 was considered because it is a value easily attainable and used for this type of regenerators. For a lower effectiveness (i.e. ε=0.5), the margin is

extended at the lower limit (the limit is the cross of the exhaust gas temperature with the air temperature at the regenerator inlet).

The upper limit is obtained when the material and energy balance cannot be solved correctly by the computer program for a given loading point with a mass fraction α. It is obvious that the higher the alpha, the lower the direct flow going to the HRSG and therefore its influence will be more significant on the high-pressure steam, which must be brought to a temperature of 565 °C in the superheater area, and on the intermediate-pressure steam that goes to the reheating area.

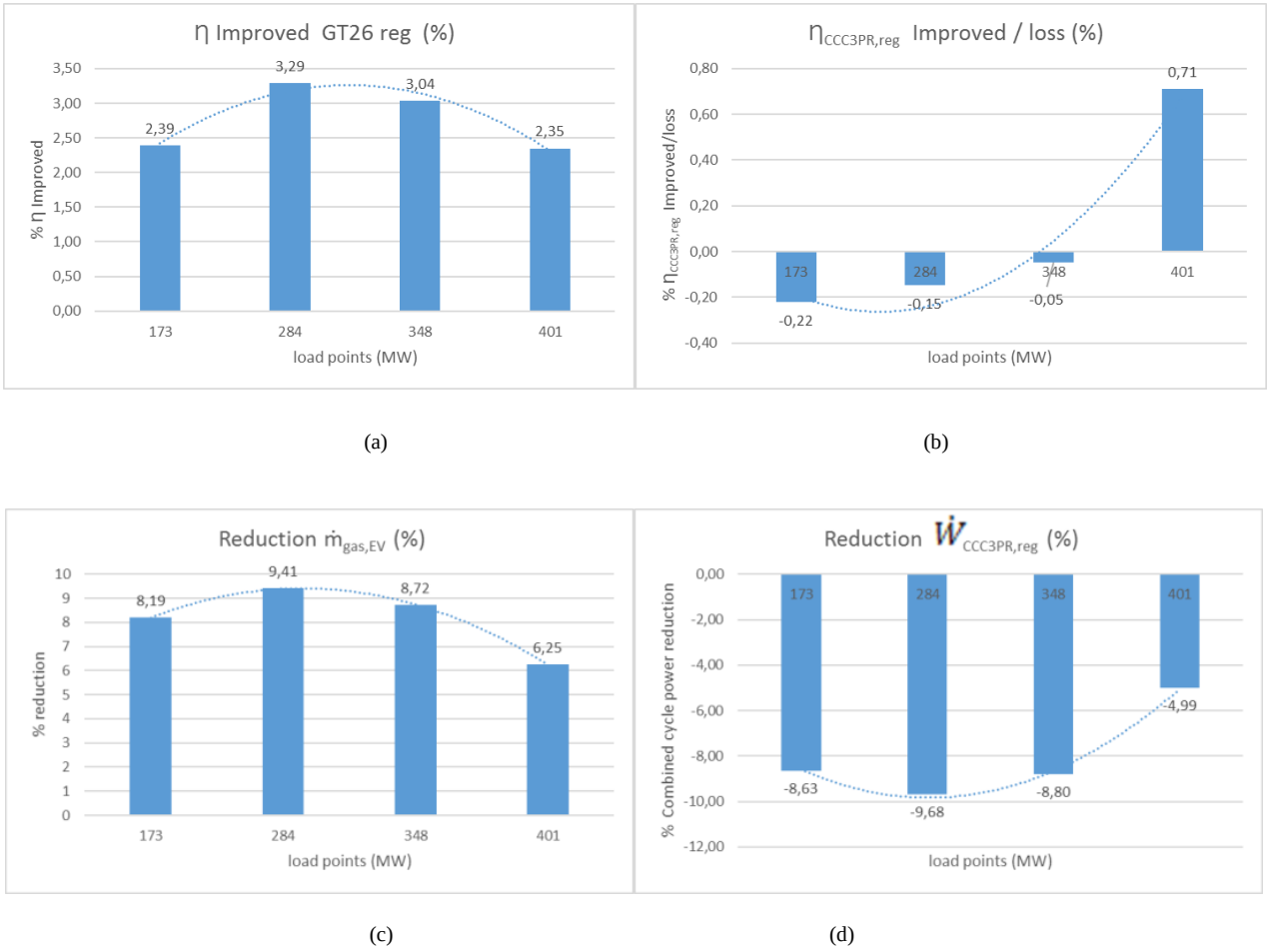

Fig. 3: (a) Improvement of η GT26 with regenerator vs loading point; (b) Improvement / loss $\eta_{CCC3PR,\,reg}$ vs loading point; (c) Reduction of gas mass flow stage EV GT26 vs loading point; (d) Power reduction in $CCC_{3PR,\,reg}$ vs loading point (by own elaboration).

The results and trends represented in Fig. 3 demonstrate how the performance of the gas turbine improves, with the introduction of the regenerator, between 2 and 3 % in turbine efficiency. With a regeneration effectiveness of 0.7, this translates into a decrease in fuel consumption in the EV fuel chamber between 6.25 and 9.41%, depending on the loading point (see Fig. 3c). In Fig. 3b and Fig. 3d the power loss of the steam cycle is shown to be compensated for by maintaining the global cycle efficiency. The decrease of the overall cycle efficiency is almost negligible in some cases. The efficiency of the combined cycle is kept practically constant with the regeneration (-0.22 to 0.71 % lower or higher) at the expense of a power loss of the steam cycle (4.99% to 9.68%) caused by the loss of temperature at the HRSG entrance.

Increasing the thermal efficiency of the gas turbine by 2.35 to 3.29 % (see Fig. 4a too) results in a decrease in the operation cost due to the reduction of fuel consumption, which, in turn, reduces gas emissions (CO, CO_2, NO, NO_2).

The decrease in the gas mass flow is more significant at the intermediate loading points. This is due to the higher exhaust gas temperatures. It is possible to make better use of the alpha fraction for the regeneration of the gas turbine in the EV stage and the steam production in the steam cycle.

The performance of the combined cycle slightly improves as the alpha fraction increases (see Fig. 4b). As expected, it is at the intermediate points of load where the highest efficiency improvements and therefore the greatest fuel consumption reductions are obtained. That is why at those points, where the cycle efficiency is lower because of the higher exhaust gas temperature with lower pressure ratio in the gas turbine, it is possible to introduce partial regeneration.

However, it is at full load that the highest pressure ratio is obtained and the lowest exhaust gas temperature is reached. This last feature is crucial for the partial regeneration at the intermediate loading points in order to maintain reasonable values of the exhaust gas temperature, at the inlet of the HRSG without losing power in the steam cycle.

Finally, we must point out again that as α fraction increases the efficiency of the new cycle improves but at the expense, as it will be seen in the following section, of higher irreversibilities in the global cycle. This is not the case for the regenerative gas turbine where the effect of the exergetic losses on the global cycle is negligible.

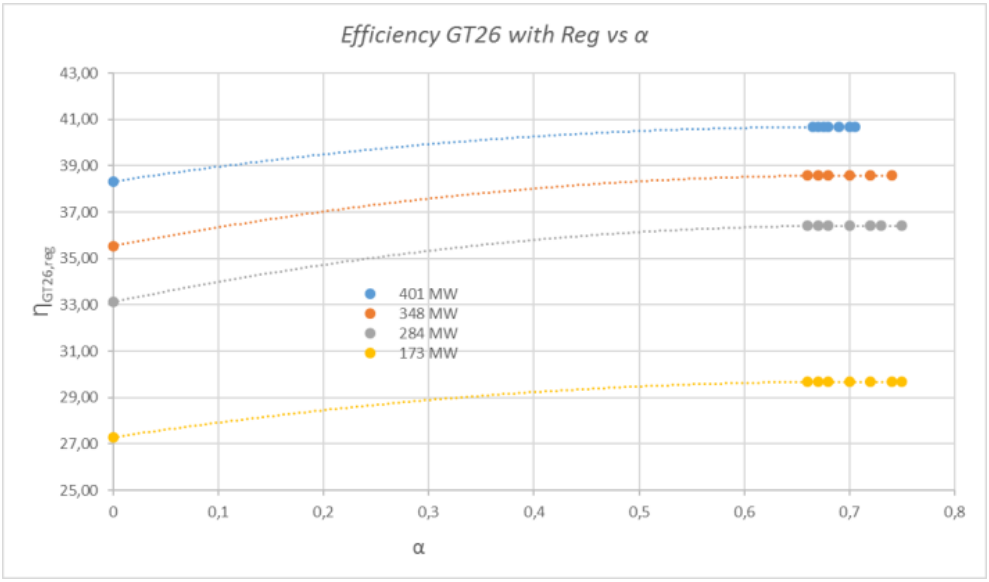

(a)

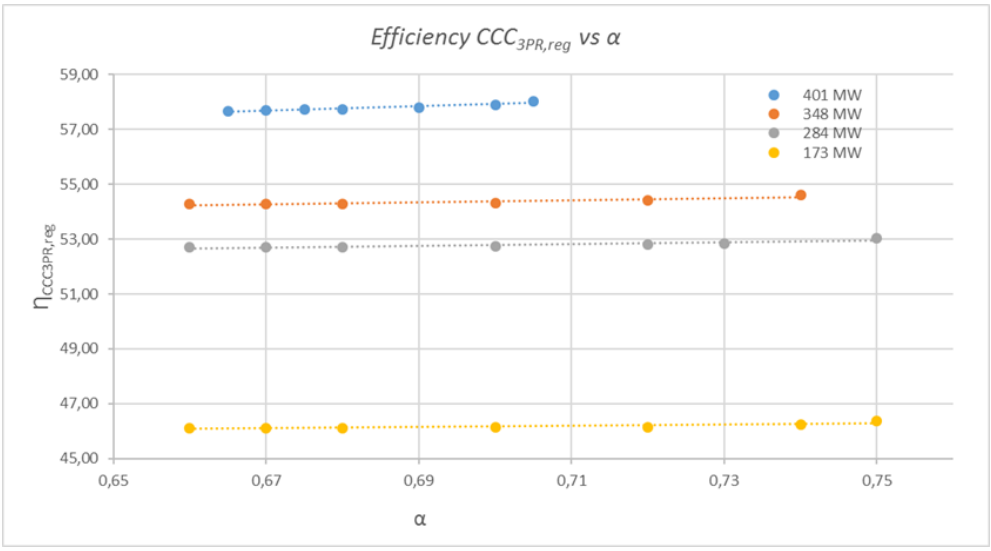

(b)

Fig. 4: (a) Variation $\eta_{GT26,\,reg}$ vs α. (b) Variation $\eta_{CCC3PR,reg}$ vs α. (Own elaboration).

Table 3: Design parameters, main results and limits of the parametric analysis for regenerative improvement in gas turbine by own elaboration.

α	r_c	$\dot{W}_{GT26}$ (MW)	$\dot{m}_{gas,EV}$ (kg/s)	$\dot{m}_{gas,SEV}$ (kg/s)	$\dot{m}_{gas,total}$ (kg/s)	% Q gas ↓↓	m_{air} (kg/s)	η_{GT26}	$T_{exhaust}$ (K)	$\dot{W}_{CV}$ (MW)	η_{CCC}	$\dot{m}_{AP}$ (kg/s)	$\dot{m}_{IP}$ (kg/s)	$\dot{m}_{BP}$ (kg/s)	$\dot{W}_{CCC}$ (MW)	$U_{a,reg}$ (kW/K)	ε	$I_{e,GT26}$ (MW)	$I_{e,CV}$ (MW)	$I_{e,total}$ (MW)	S_{reg} (m2)	Cost reg ($)
	Loading point	*173MW*																				
0	17.64	108.73	6.62	1.68	8.3		367	27.29	864	75.89	46.34	47.3	7.5	4.7	184.62	0	0	373.93	42.7	416.63	0	0
0.66	17.64	108.56	5.82	1.8	7.62	-8.19	367	29.68	862.75	60.12	46.11	40.1	8.7	5.4	168.68	9001	0.7	360.53	42.6	403.13	12859	577203
0.67	17.64	108.56	5.82	1.8	7.62	-8.19	367	29.68	862.75	60.11	46.11	40.5	8.6	5.3	168.67	4537	0.7	360.5	42.9	403.4	6481	385292
0.68	17.64	108.56	5.82	1.8	7.62	-8.19	367	29.68	862.75	60.12	46.12	41	8.5	5.2	168.68	3659	0.7	360.5	43.2	403.7	5227	339376
0.7	17.64	108.56	5.82	1.8	7.62	-8.19	367	29.68	862.75	60.17	46.13	42.3	8.3	5.1	168.73	2831	0.7	360.47	43.9	404.37	4044	291703
0.72	17.64	108.56	5.82	1.8	7.62	-8.19	367	29.68	862.71	60.23	46.15	43.7	8	5	168.79	2384	0.7	360.5	44.3	404.8	3406	263577
0.74	17.64	108.56	5.82	1.8	7.62	-8.19	367	29.68	862.71	60.57	46.24	45.9	7.6	4.7	169.13	2086	0.7	360.45	44.6	405.05	2980	243608
0.75	17.64	108.56	5.82	1.8	7.62	-8.19	367	29.68	862.71	61.05	46.37	47.8	7.3	4.5	169.61	1970	0.7	360.41	44.5	404.91	2814	235522
α	r_c	$\dot{W}_{GT26}$ (MW)	$\dot{m}_{gas,EV}$ (kg/s)	$\dot{m}_{gas,SEV}$ (kg/s)	$\dot{m}_{gas,total}$ (kg/s)	% Q gas ↓↓	m_a (kg/s)	η_{GT26}	$T_{eshaust}$ (K)	$\dot{W}_{CV}$ (MW)	η_{CCC}	$\dot{m}_{AP}$ (kg/s)	$\dot{m}_{IP}$ (kg/s)	$\dot{m}_{BP}$ (kg/s)	$\dot{W}_{CCC}$ (MW)	$U_{a,reg}$ (kW/K)	ε	$I_{e,GT26}$ (MW)	$I_{e,CV}$ (MW)	$I_{e,total}$ (MW)	S_{reg} (m2)	Cost reg ($)
	Loading point	*284 MW*																				
0	22.59	184.11	7.67	3.91	11,58		453	33,12	913	109.66	52.85	65.9	8.6	5.7	293.81	0	0	511.57	54.3	565.87	0	0
0,66	22.59	183.33	6.49	4	10,49	-9.41	453	36.41	911	82.04	52.7	50.6	11.7	7.5	265.37	9441	0.7	490.15	53.5	543.65	13487	593687
0,67	22.59	183.33	6.49	4	10,49	-9.41	453	36.41	911	82.04	52.7	51.3	11.6	7.4	265.37	5583	0.7	490.12	54	544.12	7976	435460
0,68	22.59	183.33	6.49	4	10,49	-9.41	453	36.41	911	82.05	52.7	52	11.4	7.3	265.38	4542	0.7	490.1	54.6	544.7	6489	385543
0,7	22.59	183.33	6.49	4	10,49	-9.41	453	36.41	911	82.29	52.75	53.9	11	7.1	265.62	3533	0.7	490	55.8	545.8	5047	332431
0,72	22.59	183.33	6.49	4	10,49	-9.41	453	36.41	911	82.5	52.79	56.4	10.5	6.8	265.83	2980	0.7	490.02	56.9	546.92	4257	300666
0,73	22.59	183.33	6.49	4	10,49	-9.41	453	36.41	911	82.74	52.84	58	10.1	6.6	266.07	2780	0.7	490	57.3	547.3	3971	288591
0,75	22.59	183.33	6.49	4	10,49	-9.41	453	36.41	911	83.65	53.02	62.6	9.1	6.1	266.98	2466	0.7	489.96	57.5	547.46	3523	268889
α	r_c	$\dot{W}_{GT26}$ (MW)	$\dot{m}_{gas,EV}$ (kg/s)	$\dot{m}_{gas,SEV}$ (kg/s)	$\dot{m}_{gas,total}$ (kg/s)	% Q gas ↓↓	m_a (kg/s)	η_{GT26}	$T_{eshaust}$ (K)	$\dot{W}_{CV}$ (MW)	η_{CCC}	$\dot{m}_{AP}$ (kg/s)	$\dot{m}_{IP}$ (kg/s)	$\dot{m}_{BP}$ (kg/s)	$\dot{W}_{CCC}$ (MW)	$U_{a,reg}$ (kW/K)	ε	$I_{e,GT26}$ (MW)	$I_{e,CV}$ (MW)	$I_{e,total}$ (MW)	S_{reg} (m2)	Cost reg ($)
	Loading point	*348 MW*																				
0	26.18	236.76	8.51	5.37	13.88		516	35.54	910	125.12	54.32	74.8	9.8	7.3	361.88	0	0	596.42	61.7	658.12	0	0
0.66	26.18	234.59	7.3	5.37	12.67	-8.72	516	38.57	908.3	95.46	54.27	59.2	132	9.2	330.05	9411	0.7	579.11	63.4	642.51	13444	592573
0.67	26.18	234.59	7.3	5.37	12.67	-8.72	516	38.57	908.3	95.5	54.28	60.1	13	9.1	330.09	6198	0.7	579.09	64	643.09	8854	463154
0.68	26.18	234.59	7.3	5.37	12.67	-8.72	516	38.57	908.3	95.56	54.29	61.1	12.8	9	330.15	5102	0.7	579.07	64.6	643.67	7289	412918
0.7	26.18	234.59	7.3	5.37	12.67	-8.72	516	38.57	908.3	95.77	54.32	63.5	12.3	8.7	330.36	3999	0.7	579.02	65.8	644.82	5713	357642
0.72	26.18	234.59	7.3	5.37	12.67	-8.72	516	38.57	908.3	96.31	54.41	66.9	11.5	8.3	330.9	3383	0.7	578.98	66.7	645.68	4833	324030
0.74	26.18	234.59	7.3	5.37	12.67	-8.72	516	38.57	908.3	97.46	54.59	72.5	10.3	7.5	332.05	2969	0.7	578.94	66.9	645.84	4241	300011
α	r_c	$\dot{W}_{GT26}$ (MW)	$\dot{m}_{gas,EV}$ (kg/s)	$\dot{m}_{gas,SEV}$ (kg/s)	$\dot{m}_{gas,total}$ (kg/s)	% Q gas ↓↓	m_a (kg/s)	η_{GT26}	$T_{eshaust}$ (K)	$\dot{W}_{CV}$ (MW)	η_{CCC}	$\dot{m}_{AP}$ (kg/s)	$\dot{m}_{IP}$ (kg/s)	$\dot{m}_{BP}$ (kg/s)	$\dot{W}_{CCC}$ (MW)	$U_{a,reg}$ (kW/K)	ε	$I_{e,GT26}$ (MW)	$I_{e,CV}$ (MW)	$I_{e,total}$ (MW)	S_{reg} (m2)	Cost reg ($)
	Loading point	*401 MW*																				
0	30.27	279.41	9.27	5.92	15.19		588	38.32	891	135.9	56.96	80.3	12	9.2	414.91	0	0	663.5	65.3	710.3	0	0
0.66	30.27	277.99	8.3	5.94	14.24	-6.25	588	40.67	889.7	116.2	57.67	80.6	12.2	9.1	394.19	9887	0.7	645	79.3	724.36	14124	610077
0.67	30.27	277.99	8.3	5.94	14.24	-6.25	588	40.67	889.7	116.4	57.7	81.4	12	9	394.39	7899	0.7	645.06	79.5	724.5	11284	534397
0.675	30.27	277.99	8.3	5.94	14.24	-6.25	588	40.67	889.7	116.59	57.73	82.4	11.8	8.9	394.58	6889	0.7	645	79.7	724.75	9841	492957
0.68	30.27	277.99	8.3	5.94	14.24	-6.25	588	40.67	889.7	116.57	57.72	83.2	11.6	8.8	394.56	6220	0.7	645.05	79.7	724.76	8886	464123
0.69	30.27	277.99	8.3	5.94	14.24	-6.25	588	40.67	889.7	117.15	57.81	85.8	11	8.5	395.14	5336	0.7	645.06	79.4	724.4	7623	423989
0.7	30.27	277.99	8.3	5.94	14.24	-6.25	588	40.67	889.7	117.83	57.91	89.1	10.2	8	395.82	4749	0.7	645	79.6	724.61	6784	395815
0.705	30.27	277.99	8.3	5.94	14.24	-6.25	588	40.67	889.7	118.7	58.04	92.1	9.5	7.6	396.69	4518	0.7	645.01	79.2	724.21	6454	384340

4.2. Thermodynamic analysis performance with regeneration in GT26 and solar hybridization in steam cycle.

As explained in the previous section, regeneration introduces many advantages but it also has a drawback; there is a loss of power in the global cycle when compared to the original configuration.

However, the contribution of the solar power hybridization in the vapor cycle, together with the partial regeneration of the gas turbine, decreases this power loss (see Fig. 5(a) y Fig. 5(b)). At some of the studied loading points, the power even improves minimally.

Similarly, the overall cycle performance loss, compared to the original configuration, decreases with the implementation of both technological improvements. The thermal power applied at each loading point is the maximum allowable that solves the matter and energy balances, within the computer simulator, and still provides consistent results.

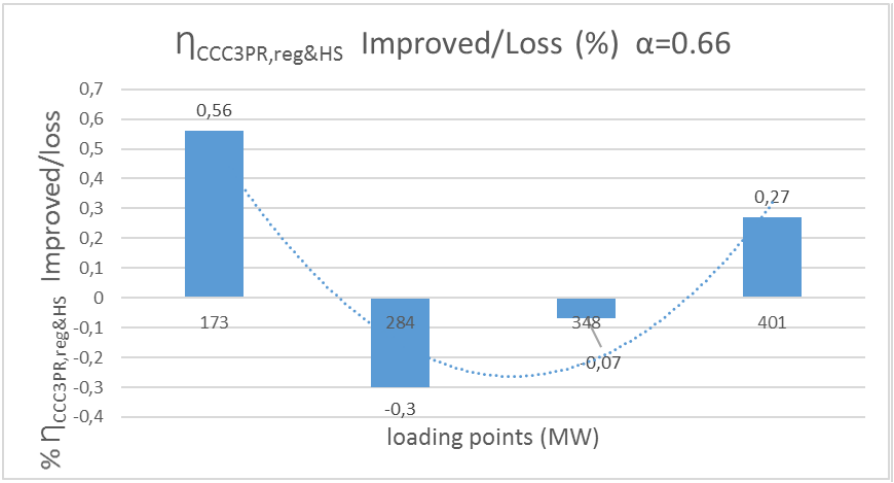

(a)

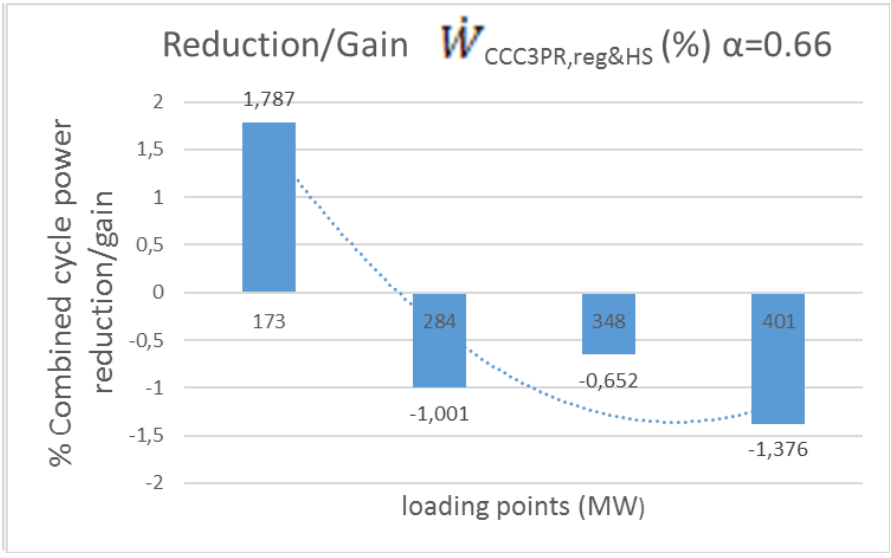

(b)

Fig. 5: (a) Improved / loss η $CCC_{3PR,\ reg\&HS}$ vs loading points. (b) Power reduction/gain $CCC_{3PR,\ reg\&HS}$ vs loading points for α=0.66 for maximum solar power absorbed by the steam cycle. (Own elaboration)

Table 4 shows the results of the multiparametric study for the configuration with regeneration and solar hybridization, for different values of Q_{solar} at each loading point. The solar power limit values obtained with the hybridization at each of the loading points, and for a given percentage of partial regeneration in the gas turbine, are also included in the table. The efficiency of the new combined cycle is kept practically the same as with regeneration only (0.56 to -0.3 % higher/lower vs -0.22 to 0.71 % lower/higher), while the power loss of the steam cycle is much lower here than with regeneration only (1.79% to -1.38% versus 4.99% to 9.68%).

Table 4: Design parameters and the main results and limits of the parametric analysis for regenerative and solar hybridization improvements in gas turbine and steam cycle respectively by own elaboration.

Loading point 173 MW

Q solar MW	ε reg	$\dot{W}_{CCC}$ (MW)	η incr solar	HR	η thermal solar	$l_{e,GT26}$ (MW)	$l_{e,CV}$ (MW)	$l_{e,total}$ (MW)	η_{CCC}
0	0.7	168.85		1.73	44.04	645	79.3	724.3	57.68
9	0.7	394.25		1.73	44.04	645	79.3	724.3	57.68
10	0.7	399.18	54.78	1.71	44.04	645	83.6	728.6	57.64
12	0.7	399.75	55,00	1.71	44.04	645	84.1	729.1	57.64
15	0.7	400.91	55.5	1.7	44.04	645	85	730	57.64
20	0.7	402.71	56.4	1.7	44.04	645	86.3	731.3	57.65
24	0.7	405.97	58.6	1.68	44.04	645	88.2	733.2	57.71
0	0.7	409.19	62.25	1.67	44.04	645	89.2	734.2	57.83
2	0.7	395.18		1.73	44.04	645	79.4	724.4	57.82
5	0.7	396.38	60,00			645	81	726	57.82
8	0.7	398.34	63.2	1.71	44.04	645	81.8	726.8	57.85
9	0.7	400.56	67.25	1.71	44.04	645	82.6	727.6	57.92
9	0.7	401.44	69.56	1.7	44.04	645	82.8	727.8	57.97
9.7	0.7	402.3	73.4	1.7	44.04	645	83	728	58.03
0	0.7	395.83		1.73		645	79.6	724.6	57.91
1	0.7	396.55	72,00	1.72	44.04	645	78.8	723.8	57.93
2	0.7	397.3	73.5	1.72	44.04	645	80	725	57.96
3	0.7	398.14	77,00	1.72	44.04	645	80.2	725.2	57.99
4	0.7	399.14	82.75	1.72	44.04	645	80.5	725.5	58.06

Loading point 348 MW

CCC C1

α	Q solar MW	ε reg	$\dot{W}_{CCC}$ (MW)	η incr Solar	HR	η thermal solar	$l_{e,GT26}$ (MW)	$l_{e,CV}$ (MW)	$l_{e,total}$ (MW)	η_{CCC}
0.66	0	0.7	332.46				579	63.4	642.4	54.67
0.66	10	0.7	337.21	47.5	1.82	44.31	579	68.9	647.9	54.55
0.66	20	0.7	342.05	47.95	1.79	44.31	579	74.3	653.3	54.45
0.66	30	0.7	347.17	49.03	1.76	44.31	579	79.4	658.4	54.4
0.66	35	0.7	349.87	49.74	1.75	44.31	579	81.8	660.8	54.4
0.66	40	0.7	352.71	50.62	1.74	44.31	579	84.2	663.2	54.42
0.66	45	0.7	355.79	51.84	1.72	44.31	579	86.3	665.3	54.47
0.66	50	0.7	359.54	54.16	1.7	44.31	579	87.8	666.8	54.63
0.7	0	0.7	332.77				579	65.9	644.9	54.72
0.7	10	0.7	337.89	51.2	1.81	44.31	579	71	650	54.66
0.7	20	0.7	343.55	53.9	1.78	44.31	579	75.6	654.6	54.69
0.7	25	0.7	346.92	56.6	1.76	44.31	579	77.5	656.5	54.79
0.7	27	0.7	348.69	58.96	1.76	44.31	579	77.8	656.8	54.9
0.74	0	0.7	334.46				579	67	646	55,00
0.74	1	0.7	335.16	70,00	1.83	44.31	579	67.3	646.3	55.02
0.74	1.5	0.7	335.52	70.67	1.83	44.31	579	67.5	646.5	55.03
0.74	2	0.7	335.91	72.5	1.83	44.31	579	67.6	646.6	55.05
0.74	2.5	0.7	336.31	74,00	1.82	44.31	579	67.8	646.8	55.07
0.74	3	0.7	336.75	76.33	1.82	44.31	579	67.9	646.9	55.1
0.74	3.7	0.7	337.47	81.35	1.82	44.31	579	68	647	55.15

Loading point 284

CCC C1

α	Q solar MW	ε reg	$\dot{W}_{CCC}$ (MW)	η incr Solar	HR	η thermal solar	$l_{e,GT26}$ (MW)	$l_{e,CV}$ (MW)	$l_{e,total}$ (MW)	η_{CCC}
0.66	0	0.7	265.37				490.15	53.5	543.65	52.7
0.66	10	0.7	270	46.3	1.86	44.6	490.15	59.1	549.25	52.58
0.66	20	0.7	274.7	46.65	1.83	44.6	490.15	64.6	554.75	52.47
0.66	30	0.7	279.54	47.23	1.8	44.6	490.15	70	560.15	52.4
0.66	40	0.7	284.89	48.8	1.77	44.6	490.15	74.9	565.05	52.42
0.66	50	0.7	290.84	50.94	1.73	44.6	490.15	79.3	569.45	52.54
0.7	0	0.7	265.62				490	55.8	545.8	52.75
0.7	10	0.7	270.41	47.9	1.86	44.6	490	61.3	551.3	52.66
0.7	20	0.7	275.64	50.1	1.83	44.6	490	66.3	556.3	52.64
0.7	30	0.7	281.97	54.5	1.79	44.6	490	70.3	560.3	52.85
0.75	0	0.7	266.98				489.96	57.5	547.46	53.02
0.75	1	0.7	267.64	66,00	1.88	44.6	489.96	59.9	549.86	53.05
0.75	2	0.7	268.34	68,00	1.88	44.6	489.96	58.2	548.16	53.08
0.75	3	0.7	269.12	71.33	1.87	44.6	489.96	58.5	548.46	53.13
0.75	4	0.7	270.07	77.25	1.86	44.6	489.96	58.6	548.56	53.21

4.3. Thermodynamic analysis, irreversibilities and cost.

In Fig. 6 the exergetic losses, extracted from Table 3, are shown for the real cycle (α=0), and for the new cycle with the improvement of partial recuperative gas turbine only. As expected, the greatest amount of exergetic losses appear in the combustion chambers of the gas turbine. The regenerator introduces an irreversibility increase in the vapor cycle as the α fraction increases. The losses increase marginally within the range of the recuperative mass flow fraction, α, of the partial regeneration. As α fraction increases, the efficiency of the new gas turbine improves but at the expense of higher overall irreversibilities of the global cycle. In the regenerative gas turbine, however, the exergetic losses hardly decrease.

The regenerator therefore introduces irreversibility both in the gas cycle and in the steam cycle. This irreversibility is negligible in the steam cycle where the reduction is around 2.4% to 3.2% at the intermediate loading points compared to the model without regenerator. However, in the gas cycle there is an increase of 4.8% to 6.5% due to the regenerator. On the other hand, the reduction of fuel consumption in the EV combustion chamber reduces the exergy losses by 2.8% to 4.2% compared to the real cycle without regenerator. Combining these, the cycle efficiency increases and the exhaust emissions decrease in comparison with the real cycle.

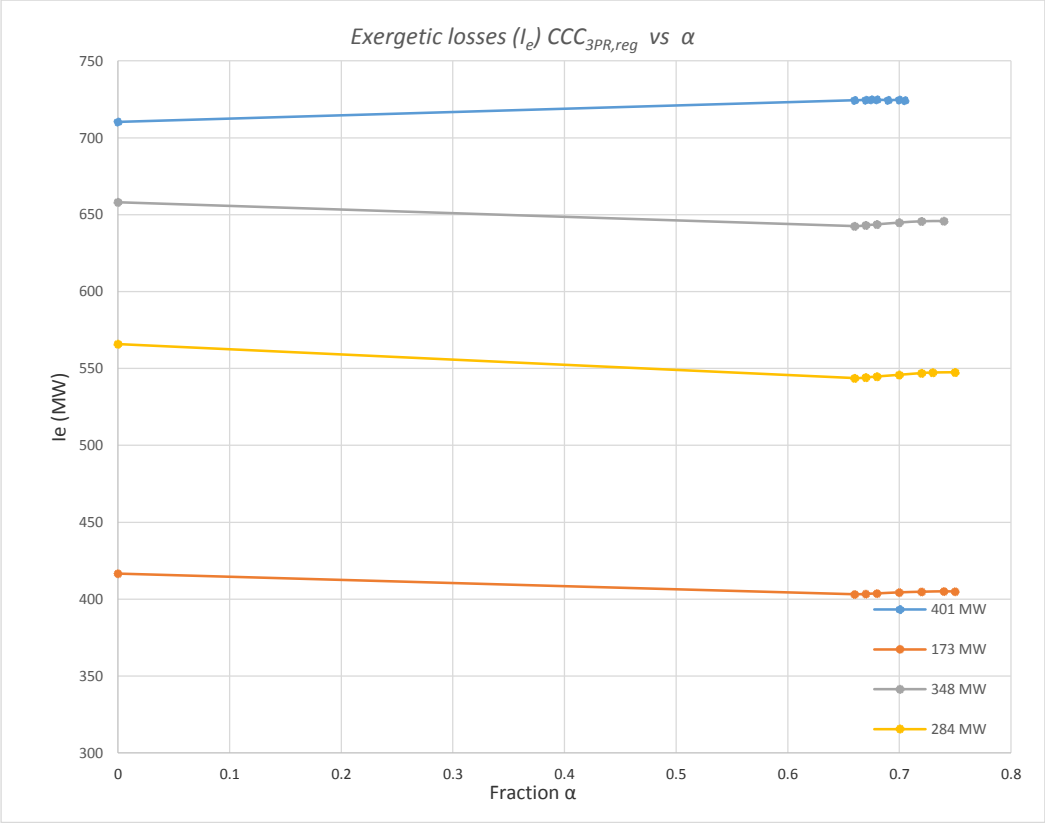

Fig. 6: Exergetic losses (I_e) $CCC_{3PR,reg}$ vs α. (Own elaboration).

Fig. 7 shows the cost evolution of the hypothetical regenerator in the new $CCC_{3PR,reg}$ cycle. The evolution, for the limits obtained at each of the loading points, indicates that the cost decreases with decreasing load and with increasing α mass fraction due to the reduction in the surface. The reason for this is that the heat capacities, the air current and the gas flow are becoming more equal as the alpha flow fraction increases. Finally, it is important to notice that the cost of the regenerator is reasonable due to its reduced size. Effectively the thermal jump, temperature range around 100 to 150 ºC, which can be applicated in intermediate loading points because of partial regeneration, is not high which implies that the surface and therefore the final cost of the hypothetical regenerator, will not elevated.

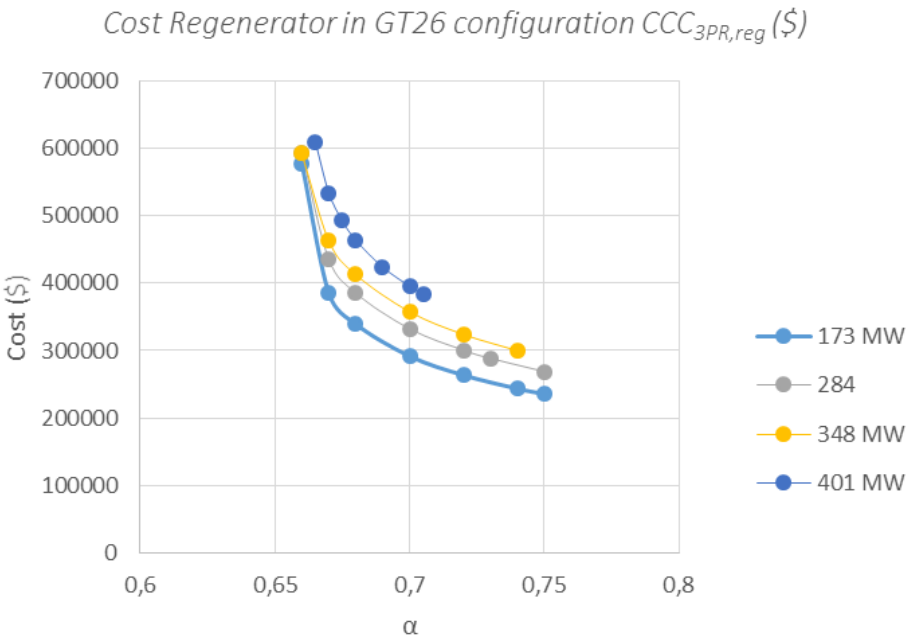

Fig. 7: Regenerator cost in GT26 configuration $CCC_{3PR,reg}$ vs gas exhaust fraction mass to regenerator. (Own elaboration).

The model calculates the required UA surface of the regenerator in each of the simulations. Their cost, in US$, has been estimated using equation 19 [65] in Appendix A.4 and assuming an overall heat transfer coefficient of 0.7 $kW \cdot m^{-2}$.

As already mentioned, the second technological improvement has a positive effect on the power of the new cycle. Nevertheless, solar hybridization increases the irreversibility of the steam cycle at the intermediate loading points (Fig. 8). This increase is around 0.63% to 1.32% with respect to the real cycle and around 3.8% to 4.75% compared to the configuration with partial regeneration only.

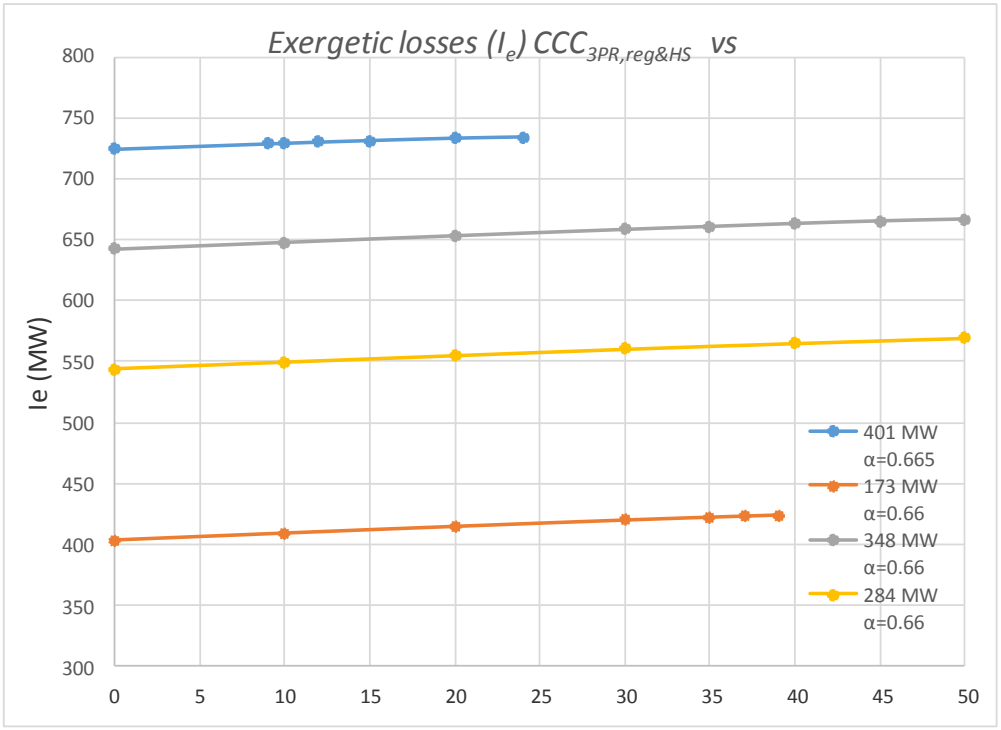

Fig. 8: Exergetic losses (I_e) $CCC_{3PR,reg\&HS}$ vs Q_{solar} (α=0.66 approximately for all loading points). (Own elaboration).

The exergy losses shown in Fig. 8, extracted from Table 4, were obtained for a partial regeneration rate α=0.66, within the limits obtained for partial regeneration at each of the loading points, with the highest possible amount of solar thermal power that would still provide consistent results. Therefore at one of the loading points, it was not possible to

introduce 50 MW of thermal power. Instead, we used the maximum value that solves the material and energy balances of the new configuration in the computer simulation.

We must keep in mind that the configuration with regeneration induces a reduction of exergetic losses with respect to the real model. Even so, the increase in irreversibility generated by the solar hybridization of the steam cycle is minimal and it is compensated by the fact that the thermal efficiency of the hybridized combined cycle is much higher than the purely solar plants working nowadays (44% vs 30%, see Table 4). It is necessary to mention that both technological improvements introduce irreversibilities in both the gas turbine and the steam cycle. This may require a more comprehensive calculation, genetic algorithm for example, before the implementation of the suggested modifications in the combined cycle, should this proposal be approved. The exhaustive parametric study in this loading points is enough to show that the partial regeneration in the gas turbine (Brayton cycle) coupled to the solar hybridization (of the heat recovery boiler within the Rankine cycle) is fully valid. On the other hand, the reduction of fuel consumption translates into the reduction of emissions and should be constrained, in economic costs, with the loss of electrical power that will be experienced by the steam cycle. This electrical power loss, as already mentioned, can be avoided and improved with the introduction of new solar thermal power.

5. Conclusions

This paper presents a thorough parametric study comparing an existing combined cycle and a hypothetical improved configuration of the same with a regenerative gas turbine and with solar hybridization in the steam cycle.

The parametric study showed that adding regeneration at different loading points of the combined cycle with triple pressure and reheating and with a partially regenerative gas turbine GT26, results in the increase of the thermal efficiency of the gas turbine and of the global cycle. This overall outcome is achieved despite a decrease in the exhaust gas temperature and a decrease in the power of the steam cycle due to a lower heat output in the regeneration of the gas cycle. In order to minimize this power loss, a second technological improvement was also introduced into the new cycle. Thanks to the integration of solar hybridization in the steam cycle in the high pressure level, the power loss is reduced from 9% to 1% at intermediate loading points.

Increasing the regeneration effectiveness results in an increase in the output power and thermal efficiency of the gas turbine cycle. The reduction of fuel consumption, with partial regeneration in the gas turbine, is significant. For a regeneration effectiveness of 0.7, it is around 6.25% to 9.45%, depending on the load. The efficiency of the combined cycle is practically maintained (-0.22 to 0.71 % lower/higher) in spite of a power loss of the steam cycle (4.99% to 9.68%) caused by the loss of temperature at the HRSG entrance.

If both of the proposed improvements; regeneration in the gas turbine and solar hybridization in the steam cycle, are added to the new configuration, the power loss is smaller (0.63% to 3.36%) and the global efficiency even increases as compared to the original (0.56 to -0.03 % higher/ lower depending on the load), for a regeneration effectiveness of 0.7 and α=0.66.

The obtained increase of the gas turbine thermal efficiency (2.35 to 3.29 % higher), results in a decrease in the operation costs by reducing the fuel consumption, and consequently, reduces the gas emissions (CO, CO_2, NO and NO_2).

The cost of the regenerator is acceptable due to its reduced size (temperature range is around 100-150 ºC). The thermal jump, which could be assumed in intermediate loading points in intermediate loading points in due to partial regeneration, is not very high. It implies that the surface and, therefore, the final cost of the hypothetical regenerator, is not very high. It is necessary to mention that both technological improvements introduce irreversibilities in both the gas turbine and the steam cycle. The efficiency of the regenerative CCGT configuration improves but at the expense of higher overall irreversibilities of the global cycle. In the regenerative gas turbine, however, the exergetic losses hardly decrease. These values are not significant. The introduction of hybridization with heat power in the steam cycle of the regenerative CCGT produces too higher irreversibilities in the global cycle which increases with the amount of heat introduced in the cycle. Even so, the increase in irreversibility generated by the solar hybridization of the steam cycle is minimal and it is compensated by the fact that the thermal efficiency of the hybridized combined cycle is much higher than the purely solar plants working nowadays (44% vs 30% approximately). However, the reduction of gas in the EV combustion chamber due the partial regeneration causes a decrease in exergy losses and in exhaust emissions in the gas turbine of both new configurations. In addition, the possible solar hybridization with thermal power from renewable energies would contribute to the loss of power due to partial regeneration in the gas turbine. The reduction of gas consumption was between 6.25% and 9.45% and the overall cycle efficiency loss is minimal due to hybridization. There was a loss of the net power of the new cycle but it is considerably lower if heat from a renewable source is supplied to the cycle. This net power loss has an average value of 7.5% with regeneration only and of 1% with regeneration and hybridization.

At intermediate loading points, where exist excess temperature not used at the outlet of the gas turbine, the partial regeneration with solar hybridization is fully admissible and recommended and would offer several advantages. Consequently, and even though the investment in the existing combined cycles would not be very high, the costs of the

fuel saved and the tons of CO_2 avoided would be considerable (approximately 4 million EUR and 26,167 t of CO_2 for a capacity factor about 40% actually in the existing CCGT's).

Acknowledgements

Thanks are due to the Energetic Engineering Department of the Technical School of Industrial Engineering UNED and the I+D+I Department of EDP Energy for providing technical support, the first, and a great amount of data of their combined cycles and financial support the second.

References

[1] Cuviella-Suárez C, Colmenar-Santos A, Castro-Gil M. Tri-generation system to couple production to demand in a combined cycle. Energy 2012;40:271-290.

[2] Borge-Díez D, Colmenar-santos A, Pérez-Molina C, Castro-Gil M.Experimental validation of a fully solar-driven triple-state absorption system in small residential buildings. Energy and Buildings 2012;55(11):227-237.

[3] R. Schultz, R. Bachmann, KA24-1CST Market Success for a Standardized Power Plant, ABB Internal Report, 1999.

[4] Variny M, Mierka O. Improvement of part load efficiency of a combined cycle power plant provisioning ancillary services. Appl Energy 2009;86:888-894 .

[5] Franco A, Casarosa C. Thermoeconomic evaluation of the feasibility of highly efficient combined cycle power plants. Energy 2004;29:1963-1982.

[6] Tica A, Gueguen H, Dumur D, Faille D, Davelaar F. Design of a combined cycle power plant model for optimization. Appl Energy 2012; 98:256-265

[7] Franco A, Casarosa C. On some perspectives for increasing the efficiency of combined cycle power plants. Appl Energy 2002; 22:1501-18.

[8] Ponc Arrieta F.R, Silva Lora E.E. Influence of ambient temperature on combined-cycle power-plant performance. Appl Energy 2005;80:261-272.

[9] Franco A, Russo A. Combined cycle plant efficiency increase based on the optimization of the heat recovery steam generator operating parameters. Int J Therm Sci 2002;41:843-59.

[10] Olivenza-León D, Medina A, Calvo Hernández A. Thermodynamic modeling of a hybrid solar gas-turbine power plant. Energy Convers Manage 2015;93:435-447.

[11] Carapellucci R. A unified approach to assess performance of different techniques for recovering exhaust heat from gas turbines. Energy Convers Manage 2009;50(5):1218-1226.

[12] Carcasci C, Facchini B. Comparison between two gas turbine solutions to increase combined power plant efficiency. Energy Convers Manage 2000;41:757–73.

[13] Bassily AM. Enhancing the efficiency and power of the triple-pressure reheat combined cycle by means of gas reheat, gas recuperation, and reduction of the irreversibility in the heat recovery steam generator. Appl Energy 2008;85:1141-62.

[14] Bassily AM. Numerical cost optimization and irreversibility analysis of the triple-pressure reheat steam-air cooled GT commercial combined cycle power plants. Appl Therm Eng 2012;40:145–60.

[15] Bassily AM. Modeling, numerical optimization, and irreversibility reduction of a dual-pressure reheat combined-cycle. Appl energy 2005;80:127-151.

[16] Sanjay Mohapatra AK. Thermodynamic assessment of impact of inlet air cooling techniques on gas turbine and combined cycle performance. Energy 2014;68:191-203.

[17] Rao A.D, Francuz D.J. An evaluation of advanced combined cycles. Appl energy 2013; 102:1178-1186.

[18] Cheng Yang C, Yang Z, Cai R. Analytical method for evaluation of gas turbine inlet air cooling in combined cycle power plant. Appl energy 2009; 86:848-856.

[19] Kotowicz J, Job M, Brzęczek M. The characteristics of ultramodern combined cycle power plants. Energy 2015 [in press]. http://dx.doi.org/10.1016/j.energy. 2015.04.006.

[20] Polyzakis AL, Koroneos C, Xydis G. Optimum gas turbine cycle for combined cycle power plant. Energy Convers Manage 2008;49(4):551–63.

[21] Rovira A, Sánchez C, Muñoz M. Analysis and optimization of combined cycles gas turbines working with partial recuperation. Energy Convers Manage 2015;106:1097-1108.

[22] Gogoi TK. A combined cycle plant with air and fuel recuperator for captive power application, Part 1: performance analysis and comparison with nonrecuperated and gas turbine cycle with only air recuperator. Energy Convers Manage 2014;79:771–7.

[23] Gogoi TK, Das TK. A combined cycle plant with air and fuel recuperator for captive power application. Part 2: inverse analysis and parameter estimation. Energy Convers Manage 2014;79:778–89.

[24] Cao Y, Gao Y, Zheng Y, Dai Y. Optimum design and thermodynamic analysis of a gas turbine and ORC combined cycle with recuperators. Energy Convers Manage 2016;116:32-41.

[25] Colmenar-Santos A, Bonilla-Gómez JL, Borge-Diez D, Castro-Gil M. Hybridization of concentrated solar power plants with biogas production systems as an alternative to premiums: The case of Spain, Renewable and Sustainable Energy Reviews 2015;47:186-197.

[26] Omar B, Kellaf A, Mohamedi K, Belhamel M. Instantaneous performance of the first Integrated Solar Combined Cycle System in Algeria. Energy Procedia 2011;6:185-193.

[27] Pondini M, Colla V, Signorini A. Models of control valve and actuation system for dynamics analysis of steam turbines. Applied Energy 2017;207:208-217.

[28] Alashkar A, Gadalla M. Thermo-economic analysis of an integrated solar power generation system using nanofluids. Applied Energy 2017;191:469-491.

[29] Zhai R, Zhao M, Yang Y. Optimizing operation of a solar-aided coal-fired power system based on the solar contribution evaluation method. Applied Energy 2015;146:328-334.

[30] Li Y, Zhang N, Cai R, Yang Y. Optimization of the solar field size for the solar–coal hybrid system. Applied Energy 2013;112:727-736.

[31] Zhao Y, Hong H, Jin H. Optimization of the solar field size for the solar–coal hybrid system. Applied Energy 2017;185(2):1162-1172.

[32] Peng S, Hong H, Wang Y, Wang Z, Jin H. Off-design thermodynamic performances on typical days of a 330MW solar aided coal-fired power plant in China. Applied Energy 2014;130:500-509.

[33] Pantaleo A, Camporeale S, Miliozzi A, Russo V, Shah N. et al. Novel hybrid CSP-biomass CHP for flexible generation: Thermo-economic analysis and profitability assessment. Applied Energy 2017;204:994-1006.

[34] González-Portillo LF, Muñoz-Antón J, Martínez-Val JM. An analytical optimization of thermal energy storage for electricity cost reduction in solar thermal electric plants. Applied Energy 2017;185(1):531-546.

[35] Montes M.J, Rovira A, Muñoz M.J, Martínez-Val M. Performance analysis of an Integrated Solar Combined Cycle using Direct Steam Generation in parabolic trough collectors. Appl Energy 2011;88:3228-3238.

[36] Dersch J, Geyer M, Herrmann S, Jones S.A, B. Kelly B, et al. Trough integration into power plants d a study on the performance and economy of integrated solar combined cycle systems. Energy 2004;29:947-959.

[37] Behar O, Khellaf A, Mohammedi K, Ait-Kaci S. A review of integrated solar combined cycle system (ISCCS) with a parabolic trough technology. Renewable and Sustainable Energy Reviews 2014;39:223-250.

[38] Nezammahalleh H, Farhadi F, Tanhaemami M. Conceptual design and techno-economic assessment of Integrated Solar Combined Cycle System with DSG technology. Sol. Energy 2010;84:1696-1705.

[39] Hosseini R, Soltani M, Valizadeh G. Technical and economic assessment of the integrated solar combined cycle power plants in Iran. Renew. Energy 2005;30:1541-1555.

[40] Baghernejad A, Yaghoubi M. Exergy analysis of an Integrated Solar Combined Cycle System. Renew. Energy 2010;35:2157-2164.

[41] Horn M, Führing H, Rheinländer J. Economic analysis of integrated solar combined cycle power plants. A sample case: the economic feasibility of an ISCCS power plant in Egypt. Energy 2004;29:935-945.

[42] Rovira A, Montes M.J, Varela F, Gil M. Comparison of Heat Transfer Fluid and Direct Steam Generation technologies for Integrated Solar Combined Cycles. Appl Thermal Engineering 2013;52:264-274.

[43] Martinez-Val JM, Montes MJ, Valdes M, Rovira A, Amengual RR. Universidad Nacional de Educación a Distancia (UNED). Sistema de regeneración parcial de turbina de gas de ciclo combinado con una o varias fuentes de calor. P201000271; 2012 Nov 9. [in Spanish].

[44] Farris R, Skowronski MJ. Method and system integrating combined cycle power plant with a solar Rankine power plant. United States patent US 20060260314 A1. 2006 Nov 23.

[45] Wei W. Zhang L. General Electric Company. Hybrid concentrated solar combined cycle power plant and solar reformer for use therein. United States patent US 20120274078 A1. 2012 Nov 1.

[46] Kane M, Favrat D, Ziegler K, Allani Y. Thermoeconomic analysis of advanced solar-fossil combined power plants. Int. J. Appl. Thermodyn. 2000;3:191-198.

[47] Reddy V.S, Kaushik S.C, Tyagi S.K. Exergetic analysis of solar concentrator aided natural gas fired combined cycle power plant. Renew. Energy 2012;39:114-125.

[48] Popov Dimityr. An option for solar thermal repowering of fossil fuel fired power plants. Solar Energy 2011;85:344–349.

[49] Rovira A, Barbero R, Montes M.J, Abbas R, Varela F. Analysis and comparison of Integrated Solar Combined Cycles using parabolic troughs and linear Fresnel reflectors as concentrating systems. Appl Energy 2016;162:990-1000.

[50] Spelling J, Laumerta B, Franssona T. Advanced hybrid solar tower combined-cycle power plants. Energy Procedia 2014; 80:1207–1217.

[51] Li Y, Yang Y. Thermodynamic analysis of a novel integrated solar combined cycle. Appl energy 2014; 122:132-142.

[52] Tian Y, Zhao C.Y. A review of solar collectors and thermal energy storage in solar thermal applications. Appl energy 2013; 104:538-553.

[53] Li Y, Yang Y. Impacts of solar multiples on the performance of integrated solar combined cycle systems with two direct steam generation fields. Appl Energy 2015; 160:673-680.

[54] Alqahtani B.J, Patiño-Echeverri D. Integrated Solar Combined Cycle Power Plants: Paving the way for thermal solar. Appl Energy 2016; 169:927-936.

[55] Baghernejad A, Yaghoubi M. Exergoeconomic optimization of an Integrated Solar Combined Cycle System using evolutionary algorithms. International Journal of Energy Research 2011;35:601-615.

[56] James S, Favrat D, Martin A, Augsburger G. Thermoeconomic optimization of a combined-cycle solar tower power plant. Energy 2011;41:113-120.

[57] Naserian M.M, Farahat S, Sarhaddi F. Exergoeconomic multi objective optimization and sensitivity analysis of a regenerative Brayton cycle. Energy Convers Manage 2016;117:95-105.

[58] Chen L, Sun F, Wu C, Kiang R.L. Theoretical analysis of the performance of a regenerative closed Brayton cycle with internal irreversibilities. Energy Convers Manage 1997;38(9):871-877.

[59] Goodarzi, M. Comparative energy analysis on a new regenerative Brayton cycle. Energy Convers Manage 2016;120:25-31.

[60] Naserian M.M, Farahat S, Sarhaddi F. New exergy analysis of a regenerative closed Brayton cycle. Energy Convers Manage 2017;134:116-124.

[61] Anvari S, Jafarmadar S, Khalilarya S. Proposal of a combined heat and power plant hybridized with regeneration organic rankine cycle: Energy-exergy evaluation. Energy Convers Manage 2016;122:357-365.

[62] Colmenar-Santos A, Zarzuelo-Puch G, Borge-Díez D, García-Diéguez C. Thermodynamic and exergoeconomic analysis of energy recovery system of biogas from a wastewater treatment plant and use in a Stirling engine. Renewable energy 2016;88 (14):171-184.

[63] Walsh PP, Fletcher P. Gas turbine performance. 2nd ed. Oxford: BlackWell 2004.

[64] Horlock JH. Combined power plants. 1a ed. Oxford: Pergamon Press 1992.

[65] Zare V, Mahmoudi SMS, Yari M. An exergoeconomic investigation of waste heat recovery from the Gas Turbine-Modular Helium Reactor (GT-MHR) employing an ammonia–water power/cooling cycle. Energy 2013;61:397-409

Appendix A.

As mentioned in Materials and Methods 3, for this study it was necessary to obtain a computer model with Visual Basic Code, in order to simulate the existing cycle CCP_{3PR} with real data and to compare it with the improved model of $CCC_{3PR,\ reg\&HS}$. The way to obtain the models from the data of the existing plant is shown in Fig. *9* (already included in Appendix A). A software has been obtained to represent reliably the values of the real model (plant data) in four loading points distant from the regulation limits in which the CCGT currently is working (170 MW to 400 MW). The software has many parameters that can be easily modified to obtain the selected loading points. Once the software is set to the real model at each loading point, it is possible to include the technological improvements and compare the new values such as performances, mass flows, temperatures, etc. For this the software solves balances of matter and energy in each one of the equipment that make up the new CCGT considering the new improvements. The tables 1 to 4 are obtained for each loading point by varying parameters such as the fraction of exhaust gases to the regenerator and/or the amount of solar power supplied to the steam cycle. In this way, considering the infinite number of parameters that can be obtained from the software for each of the new configurations, the most characteristic values that would represent the new cycle are shown, such as performance, irreversibilities, efficiencies, etc.

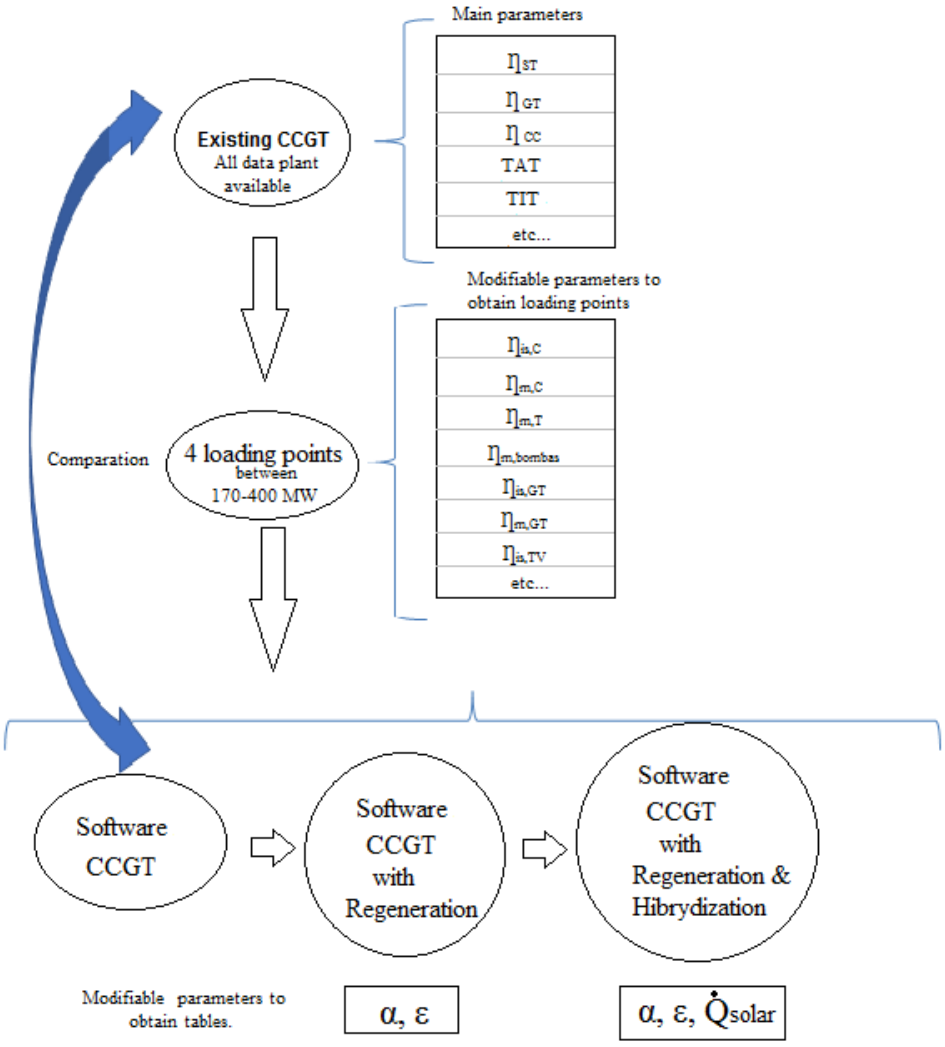

Fig. 9: Flow-chart of the software obtaining process and results for each of the configurations.

The theory to obtain computer models in the different parts of the cycle was the following:

A.1. *Theory applied to obtain the computer models: Sequential combustion gas turbine.*

The compressor, of variable geometry, is directly fed with the air from the atmosphere and compresses it adiabatically. The output pressure is determined by the inlet pressure (which is the atmospheric minus a loss of charge which has been taken into account in the computer simulation) and the compression ratio (r_c):

$$P_2 = r_c \cdot P_1 = r_c \cdot (P_{atm} - \Delta P) \quad (3)$$

Subscript 2 refers to the output state and subscript 1 to the general input in the computer simulation, it is possible to assume a loss of load, ΔP, which causes the output value to be equal to the values obtained in the actual cycle.

If the compression was adiabatic and reversible (there would be no heat transfer, Q = 0, and therefore an iso-entropic process would occur) and if air was considered an ideal or perfect gas specific heat capacity of which does not change at constant pressure (c_P = cte,), the outlet temperature would be:

$$T_{2s} = T_1 \cdot \left(\frac{P_2}{P_1} \right)^{\frac{\gamma-1}{\gamma}} \quad (4)$$

The above equation is true for ideal gases of constant cp. However, given that correlations are used, the c_p depends on the temperature, so the isentropic point is calculated by introducing the entropy and pressure of the point in the correlations. Since this is an irreversible process, the isoentropic efficiency of the compressor would be defined as:

$$\eta_{is,c} = \left(\frac{h_{2s} - h_1}{h_2 - h_1} \right) \quad (5)$$

In the equation, the first term of equality corresponds to the specific work to be done in the process. For each loading point of the gas turbine, in addition to an air mass flow rate (m_a), within the combined cycle, an isentropic efficiency value in % can be included in the simulation model CCC_{3PR}. The exit point can be calculated by clearing from equation (5) if ideal gas is assumed (relationship between enthalpy, temperature and air pressure) being the enthalpy a function of the temperature (h = h(T)).

The power consumed by the compressor will be:

$$\dot{W}_{comp.GT} = \left(\frac{\dot{m}_a \cdot (h_2 - h_1)}{\eta_{m,c}} \right) \quad (6)$$

In equation (6), $\eta_{m,\,C}$ represents the mechanical efficiency of the compressor in which it is considered a % determined by the computer program in order to obtain each loading point.

In the first combustion chamber (EV) the gas is introduced and mixed with the air entering from the compressor. This mixture is burnt and raises its temperature to a certain value (design data for each load point) and will depend mainly on the richness of the mixture. The process is performed practically at constant pressure, although a loss of load is inevitable, and in the computer simulation of the models, that value was estimated in the pressure at the inlet and outlet, $P_{out} = P_{in} + \Delta P$. The equation that models the process is as follows in equation (7):

$$\dot{m}_a \cdot h_1 + \dot{m}_f \cdot LHV \cdot \eta_{c.comb} = (\dot{m}_a + \dot{m}_f) \cdot h_2 \quad (7)$$

Where the generic h_1 corresponds to the input of the combustion chamber. The value of h_2 is known, since the temperature value at the exit of the combustion chamber is a design parameter (turbine inlet temperature). In the computer simulation an efficiency design value in the combustion chamber η_{CComb} = 98% is established. The value of the calorific value of the fuel is set at LHV = 48000 kJ / kg, which corresponds to the lower calorific value of the natural gas (methane). On the other hand, the dosing is defined in equation (8) as:

$$F = \frac{\dot{m}_f}{\dot{m}_a} \tag{8}$$

That can be calculated by clearing from equation (7). We must emphasize that the composition of the gases should be considered different from the air, since this factor is important when establishing its specific heat. In the computer simulation, the calculation of the dosing was done by firstly assuming a value of dosing (1/50) and afterwards using a loop iteration until getting the value of the dosing on the basis that the air flow is the one corresponding to the Point of work or load to be simulated (function of the geometric variables blades, VGV's, and atmospheric conditions of pressure and temperature).

The gases exiting the EV chamber expand to a certain pressure (about half the r_c) and a temperature (TAT_{HP}) and pass to the second chamber (SEV) where they are again heated to a temperature so that the temperature (TAT_{LP}) is a known value. In this chamber the computer model again applies an iteration loop, knowing the isoentropic efficiency of said stage and the TAT_{LP}, so that the model can converge and calculate the mass expenditure at that point and the entry temperature in the SEV.

Lastly; the gases, which leave the second combustion chamber, are introduced into the turbine or expansion chamber, where they expand adiabatically to a known pressure, which, as already mentioned, will be slightly higher than the atmospheric pressure.

In a similar way to the one in the compressor, for both EV and SEV expansion chambers, if the expansion were adiabatic and reversible (where there would be no heat transfer, Q = 0, and therefore an iso-entropic process), and if air is considered an ideal gas specific heat capacity of which does not change at constant pressure (c_p = cte, or also called perfect gas), the outlet temperature, showed in equation (9), would be:

$$T_{4s} = T_3 \cdot \left(\frac{P_4}{P_3} \right)^{\frac{\gamma-1}{\gamma}} \tag{9}$$

As shown before, the expression is only valid for ideal gases of constant c_p. As it is considered temperature dependent, the corresponding pressure and entropy are introduced into the correlations.

The isoentropic efficiency of the turbine would be defined as:

$$\eta_{is,t} = \left(\frac{h_4 - h_3}{h_3 - h_{4s}} \right) \tag{10}$$

The subscript 4, in equation (10) corresponds to the output and 3 to the input in general, and $\eta_{is,t}$ is the isentropic efficiency of the turbine (in EV and SEV), which can be changed and adapted, as a design data, in the computer tool at the load point that makes the real values could be used in the simulation model at that point. Furthers details will be discussed and shown in the results section of the simulation model.

As in the compressor the power is calculated with the following equation (11):

$$\dot{W}_{t.GT} = \dot{m}_g \cdot (h_2 - h_1) \cdot \eta_{m,t}, \tag{11}$$

Where $\eta_{m,t}$ is the mechanical efficiency of the turbine (value in % changeable in the simulation model of each of the four configurations and at each loading point) and m_G the mass flow rate of the exhaust gas at the outlet of the first chamber (air flow + fuel flow). For the second SEV chamber the above formulas apply.

For the calculation of the regenerator, the effectiveness of the regenerator must be taken into account, to calculate the new air temperature prior to entering the combustion chamber EV. A balance to the regenerator will give us the outlet temperature of the exhaust gases that will go to the HRSG. Equation (12) defines effectiveness as:

$$\varepsilon_{reg} = \left(\frac{T_{in,gas} - T_{out,gas}}{T_{in,gas} - T_{in,air}} \right), \tag{12}$$

For the resolution of the regenerator inside the gas turbine, it will be necessary to make in it one mass and energy

balance taking into account the value of partial regeneration, α. With this values it will be possible to obtain the outlet temperature of exhaust gases for a fixed value of effectiveness. The calculation of the surface of the exchanger is carried out by means of the computer program, taking into account the factor UA, product of the overall heat-transfer coefficient and the heat exchange area, in ($W \cdot K^{-1}$). One of the key factors needed to follow is the pressure drop that the recuperative configuration introduces in the air side (additionally to that in the combustion chamber) and in the HRSG. In fact, the higher the heat exchange area of the recuperator, the higher the pressure drop [63] .

A.2. *Theory applied to obtain computer models: Steam cycle*

For the resolution of the steam cycle coupled to the regenerative gas turbine, it will be necessary to consider the material and energy balances in each of the sections in which the HRSG is divided in addition to the current α and 1- α that go to the AP evaporator zone and to the entrance of the HRSG, respectively. In addition, it will be necessary to know the amount of solar heat that is introduced in the high pressure evaporator, 0 to 50 MW thermal (see equations system 13).

Superheater (SB_{AP}):	$\dot{m}_{G,1-\alpha}\cdot(h_{G1} - h_{G2}) = \dot{m}_{v,AP}\cdot(h_{A1} - h_{A2})$
Reheater (Rh):	$\dot{m}_{G,1-\alpha}\cdot(h_{G2} - h_{G3}) = \dot{m}_{v,rc}\cdot(h_{I1} - h_{I2})$
Evaporator (EV_{AP}):	$\dot{m}_{G}\cdot(h_{G3,\alpha+1-\alpha} - h_{G4}) + \dot{Q}_{solar} = \dot{m}_{v,AP}\cdot(h_{A2} - h_{A3})$
Superheater (SB_{IP}):	$\dot{m}_{G}\cdot(h_{G4} - h_{G5}) = \dot{m}_{v,IP}\cdot(h_{I4} - h_{I5})$
Economizator ($EC3_{AP}$):	$\dot{m}_{G}\cdot(h_{G6} - h_{G7}) = \dot{m}_{v,AP}\cdot(h_{A3} - h_{A4})$
Evaporator (EV_{IP}):	$\dot{m}_{G}\cdot(h_{G7} - h_{G8}) = \dot{m}_{v,IP}\cdot(h_{I5} - h_{I6})$
Economizator ($EC2_{AIP}$):	$\dot{m}_{G}\cdot(h_{G8} - h_{G9}) = \dot{m}_{v,AP}\cdot(h_{A4} - h_{A5}) + \dot{m}_{v,IP}\cdot(h_{I6} - h_{I7})$
Evaporator (EV_{BP}):	$\dot{m}_{G}\cdot(h_{G9} - h_{G10}) = \dot{m}_{v,BP}\cdot(h_{B1} - h_{B2})$
Economizator (EC_{AIBP}):	$\dot{m}_{G}\cdot(h_{G10} - h_{G11}) = \dot{m}_{v,AP}\cdot(h_{A5} - h_{A6}) + \dot{m}_{v,IP+BP}\cdot(h_{I7} - h_{I8})$
Laminar:	$h_{I7} = h_{B2}$
Division:	$\dot{m}_{v,IP+BP} = \dot{m}_{v,IP} + \dot{m}_{v,BP}$
Mixture:	$\dot{m}_{v,rc} \cdot h_{I2} = \dot{m}_{v,IP} \cdot h_{I4} + \dot{m}_{v,AP} \cdot h_{I3}$
Mixture:	$\dot{m}_{v,rc} = = \dot{m}_{v,IP} + \dot{m}_{v,AP}$
Mixture:	$\dot{m}_{G}\cdot h_{G3,\alpha+1-\alpha} = \dot{m}_{G,1-\alpha}\cdot h_{G3} + \dot{m}_{G,\alpha}\cdot h_{G3\alpha}$
Mixture:	$\dot{m}_{G} = \dot{m}_{G,\alpha} + \dot{m}_{G,1-\alpha}$

(13)

A.3. *Theory applied to obtain computer models: Solar power*

As already mentioned, with the contribution of solar energy we can assess the amount of thermal power that the high pressure evaporator is able to absorb. This thermal power is translated into electrical power that improves the loss, as described in the results section, due to the partial regeneration in gas turbine.

The thermal power will be introduced at the high-pressure level because its quality and conditions so advise it [35].

In order to interpret the results obtained with the solar field, the incremental solar efficiency, thermal efficiency and heat rate have been calculated. These variables are expressed according to equations 10 to 12:

$$\eta_{incrementd\_solar} = \left(\frac{\dot{W}_{CCC_{3PR,Reg\&HS}} - \dot{W}_{Qsolar}}{\dot{Q}_{solar=50MW}} \right) \qquad (14)$$

The incremental solar efficiency is defined as the increase of power obtained in the new combined cycle when solar thermal power is introduced with respect to the real cycle ($Q_{solar=0}$).

$$\eta_{solar\_thermal} = \left(\frac{\dot{Q}_{solar\_corrected}}{\dot{Q}_{solar\_gross}} \right), \tag{15}$$

where the corrected thermal heat is a function of the raw solar heat introduced at the saturation pressure of the high pressure level.

$$HR_{CCC_{3PR,Reg\&HS}} = \left(\frac{\dot{m}_f \cdot LHV}{\dot{W}_{gas\_cyvle} + \dot{W}_{steam\_cycle}} \right) \tag{16}$$

HR parameter expresses an inverse of performance considering only the contribution of fuel. A lower value is an improvement as it means that small amount of fuel is used to produce a lot of power.

A.4. *Irreversibility and cost*

As already discussed, in addition to the comparative study of the models obtained from simulations, the exergetic losses in both models (i.e. real and improved) were calculated to see the effect of the irreversibilities.
The general formulation for the exergy balances is shown in equation 17:

$$E_{IN} = E_{OUT} - E^{Q} + W + I = T_{amb} \cdot (\dot{m}_g \cdot s_g - \dot{m}_a \cdot s_a - \dot{m}_f \cdot s_f + (\Delta S)_0) + \dot{m}_f \cdot LHV \cdot (1 - \eta_{ccomb}) \tag{17}$$

It will be necessary to consider the exergetic losses in the combustion chambers, EV and SEV, of the gas turbine and assess the effect produced by the regenerator in the new model since it is in this equipment is where higher values were obtained. It is possible to calculate the exergetic losses obtained in the real and the improved model considering equation (17) obtained after an energy balance to each of the combustion chambers jointly, and equation 18 [64], that relates the free energy of formation and the heat of combustion of a hydrocarbon and its hydrogen-carbon ratio.

$$\frac{(-\Delta G)_0}{(-\Delta H)_0} = 1 - \frac{T_0 \cdot (-\Delta S)_0}{LHV} = 1.0401 + 1.728 \cdot (h/c) \tag{18}$$

The model also will calculate the required UA surface of the regenerator in each of the simulations. Their cost, in US$, has been estimated using equation 19 [65] and assuming an overall heat transfer coefficient of 0.7 $kW \cdot m^{-2}$.

$$Rg_{cost} = 2681 \cdot A^{0.59} \tag{19}$$

A.5. *Layout of CCC_{3PR} , $CCC_{3PR,reg}$ and $CCC_{3PR,reg\&HS}$*

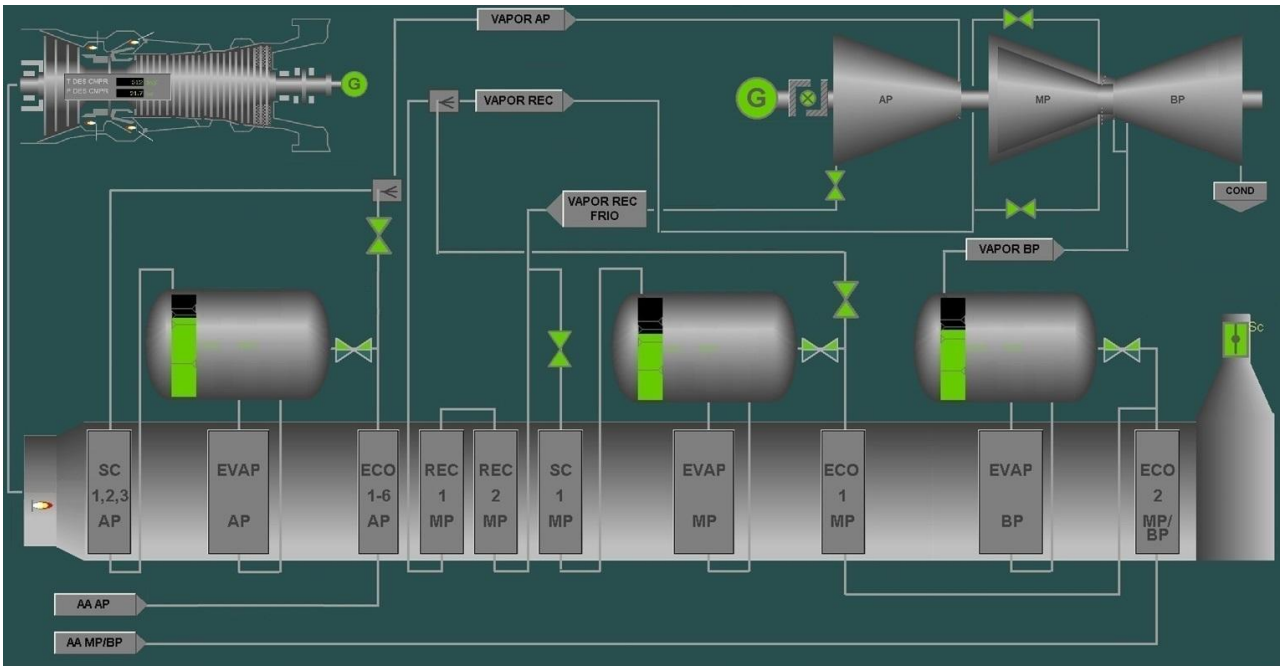

Fig. 10 Layout of the conventional CCC_{3PR}. (Own elaboration).

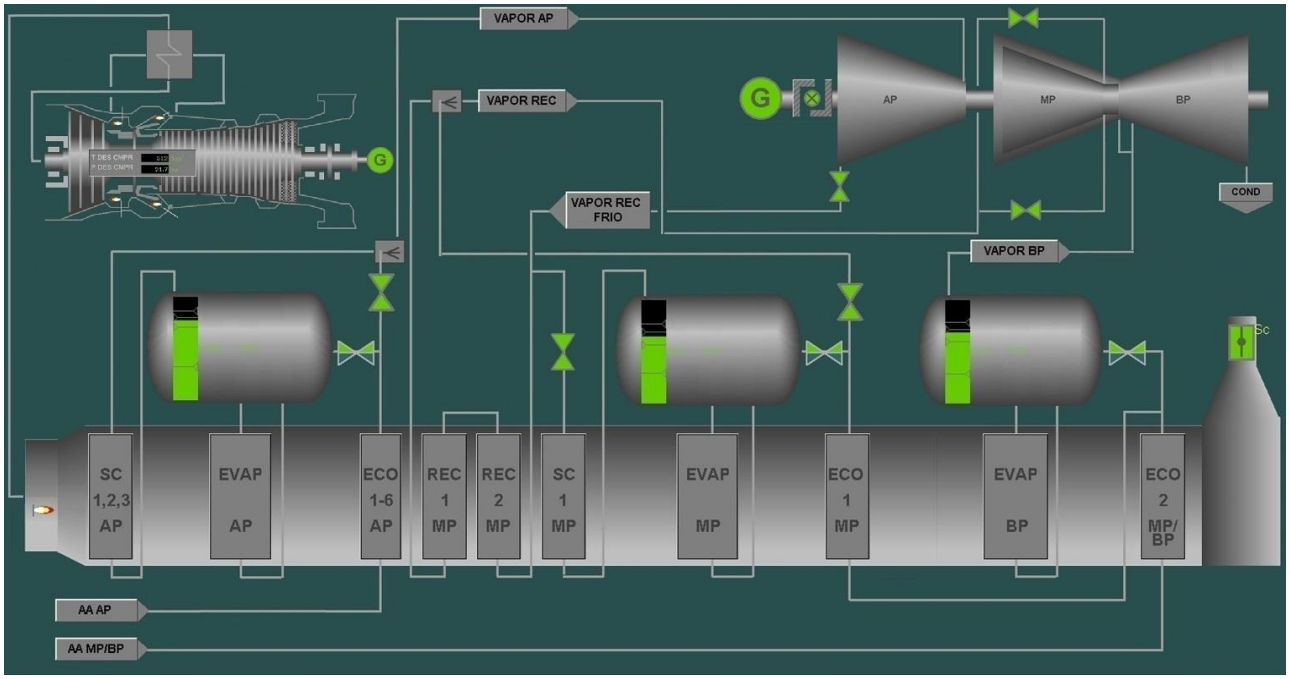

Fig. 11 Layout of the $CCC_{3PR,reg}$ with partial recuperation α. (Own elaboration).

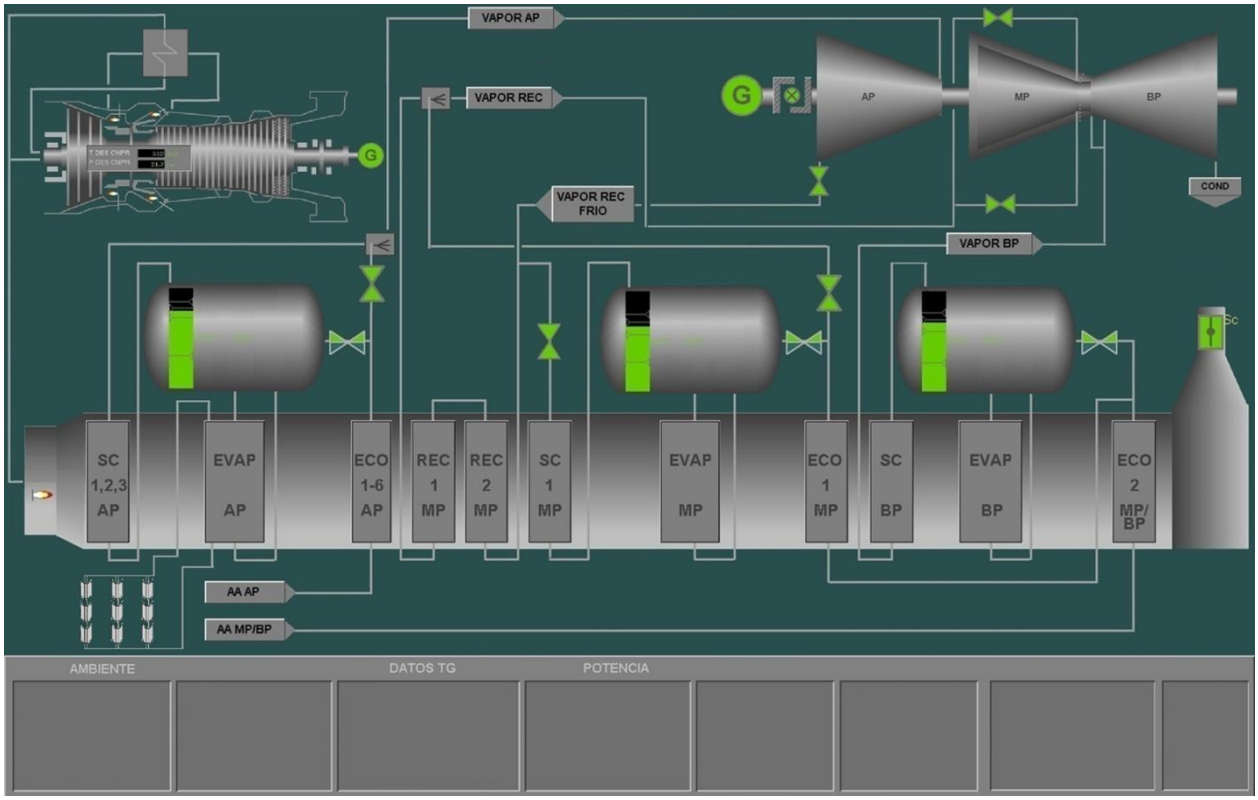

Fig. 12: Layout of the $CCC_{3PR,reg\&HS}$ with partial recuperation α and solar hybridization $\dot{Q}_{solar}$ (MW) (Own elaboration).

A.6. *Example simulation CCC_{3PR} , $CCC_{3PR,reg}$ and $CCC_{3PR,reg\&HS}$ with VB code*

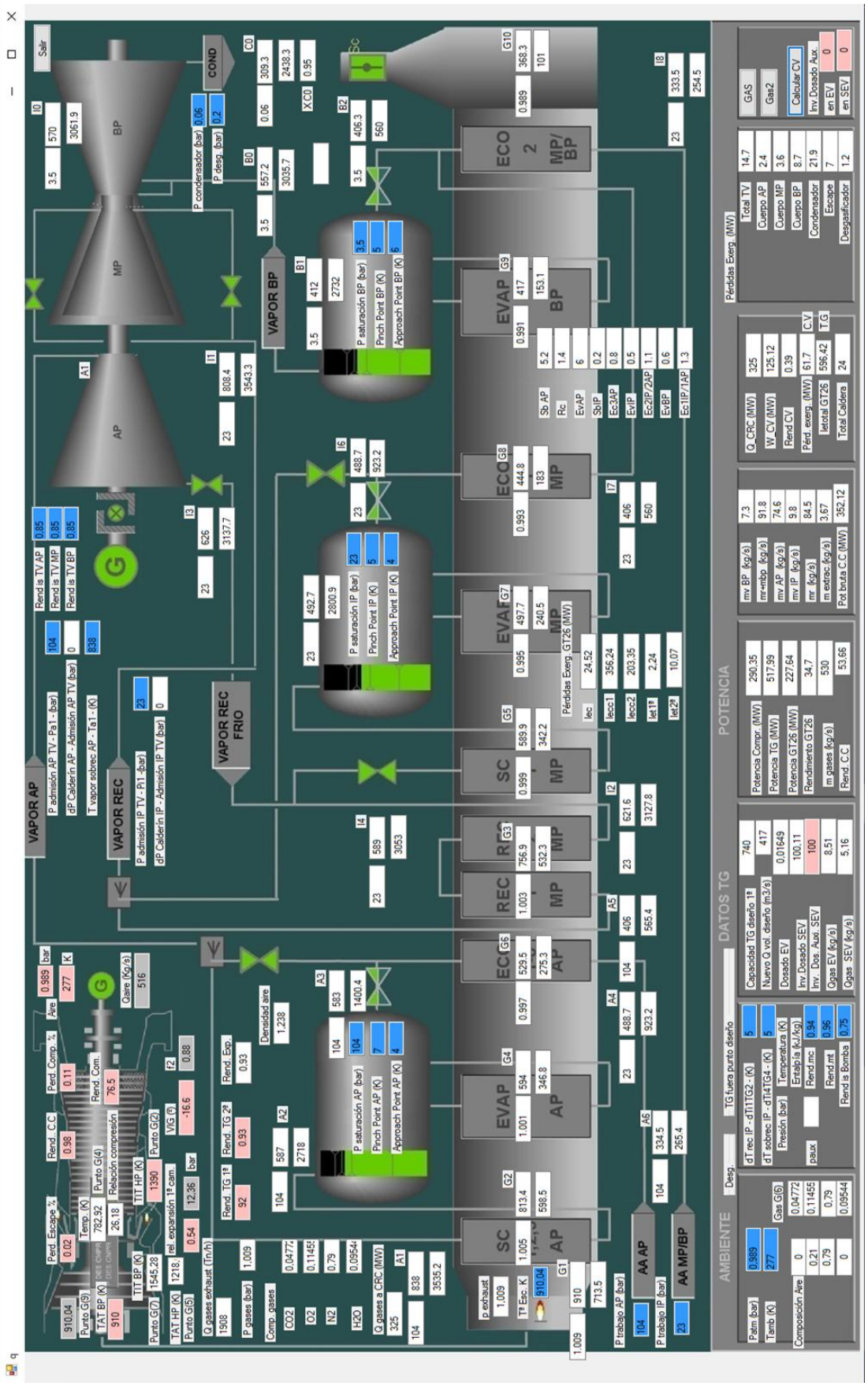

Fig. 13 Example simulation CCC_{3PR} loading point 348 MW. (Own elaboration).

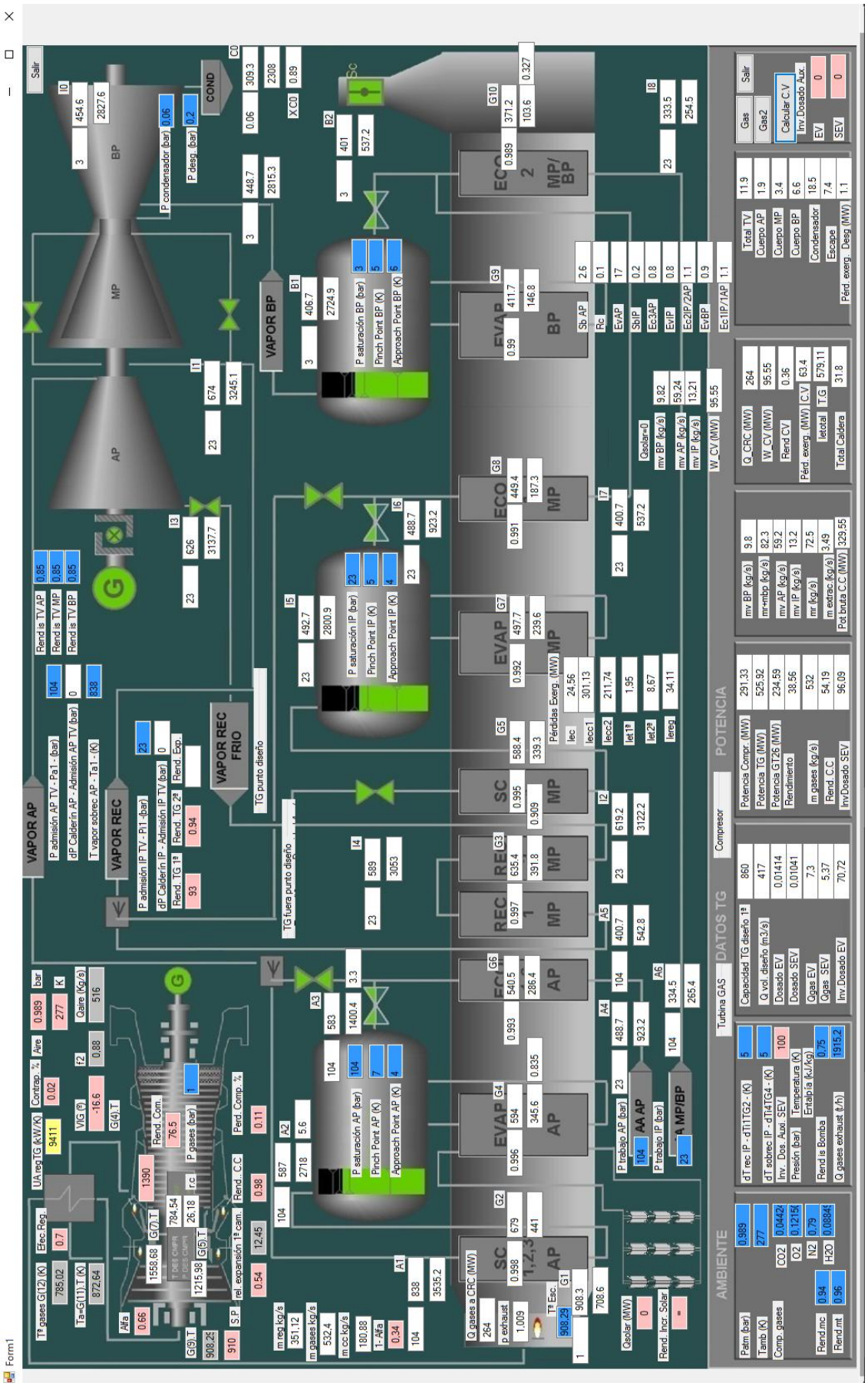

Fig. 14 Example simulation $CCC_{3PR,reg}$ loading point 348 MW α=0.66. (Own elaboration).

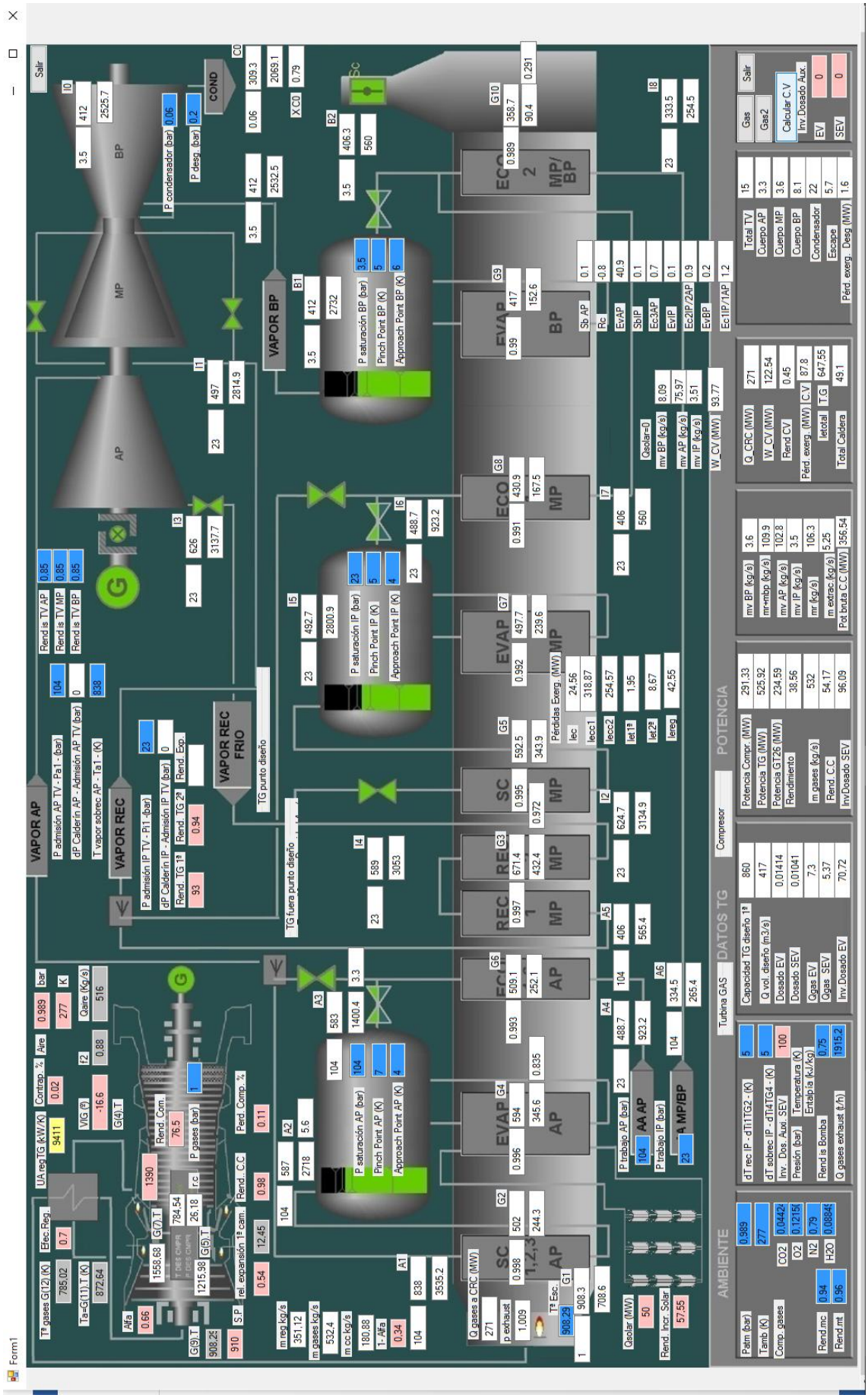

Fig. 15: Example simulation $CCC_{3PR,reg\&HS}$ loading point 348 MW α=0.66 Q=50MW. (Own elaboration).